Utrecht University

Koninklijk Nederlands
Meteorologisch Instituut
Ministerie van Infrastructuur en Milieu

Utrecht University

Institute for Marine and Atmospheric research Utrecht (IMAU)

Stratospheric warming analysis using the PV-θ view

Author:
Angelo Bohan

Supervisors:
Aarnout van Delden (UU)
Michiel van den Broeke (UU)
Michiel van Weele (KNMI)

MSc Climate Physics

November 9, 2019

Abstract

Sudden Stratospheric Warmings (SSWs) are events in which the middle stratosphere, where it is usually very cold, warms up by 30 to even 50 degrees Celcius. SSWs lead to a displacement or split of the polar vortex, a low pressure system above the Poles which is created every autumn and disappears every spring by the changing temperature differences between the equator and the poles. In many papers and literature, these stratospheric events are related to drastic changes in the general circulation in the troposphere. Increase of surface pressure at northern latitudes (negative AO and NAO) and weakening, meandering and southward displacement of the jet stream are frequently observed after a SSW.

There are accepted theories on the cause of SSWs. However, there is still much unclear how these disturbances in the stratosphere alter the general circulation in the troposphere. An SSW is defined as the reversal of the zonal mean zonal wind at a height of 10 hPa at a latitude of 60°N. One of the shortcomings of the current definition of the SSW is that it does not take the vertical extent of the event into account since it is only restricted to a height of 10 hPa. In response to the Arctic air outbreak of 2018 in Europe, KNMI published a report where an improved definition with additional requirements regarding the depth of a SSW was proposed: the Deep Stratospheric Warming (DSW). A DSW is defined as a reversal of the zonal mean zonal wind in a layer between 10-100 hPa for at least 5 days, averaged between 60-70°N. On at least 2 days, the layer thickness must be minimal 80 hPa. Since DSWs cover a much deeper layer of the stratosphere, there is a bigger chance that they influence the general tropospheric circulation significantly.

The downward propagation of perturbations coming from an SSW are investigated in this thesis. Five cases of SSWs, of which 4 cases are also DSWs, are thoroughly analyzed in order to provide an explanation for the downward effects which possibly affects the tropospheric circulation. In order to do that, the PV-θ view is used. In this view, the potential temperature is used as the vertical coordinate and the potential vorticity is the most important metric.

The disturbances caused by an SSW lead to the creation of PV anomalies. The atmosphere adjusts itself to these PV anomalies, which is actually adjustment to the thermal wind principle. By investigating the fluxes of potential vorticity in the form of isentropic mass and PVS (vorticity) flux, it turns out that before and during a SSW, the poleward mass circulation and equatorward PVS circulation in the stratosphere enhances generally. An increased poleward mass flux causes the pressure increases at northern latitudes. An increased equatorward PVS flux acts as a zonal force on the zonal wind, which decelerates the jet. The PV anomalies have a vertical reach in which they can influence the air masses: the Rossby scale height. The stratospheric PV anomalies have a Rossby height which is large enough to have influence on the troposphere.

Contents

1 Introduction

The stratosphere, roughly 10 to 50 km above the Earths surface, is something most people do not know much about, except that most of the time it is very cold there. It is therefore that stratospheric research just become popular halfway the 20th century, when the first stratospheric observations were done. Nowadays, we know that the stratosphere is an important part of the atmosphere. Important chemical reactions causing phenomena like the ozone hole take place in the stratosphere for example. It is thus very useful to understand what happens in the stratosphere, and what its connections are with the troposphere.

To show the relevance of those connections, we go back to an event which happened in February 2018. During the first days of that month, the temperature in the stratosphere above the North pole increased by more than 30 degrees within a few days. This is a phenomenon called Sudden Stratospheric Warming (SSW). The winter in Northern Europe was very mild so far, but the end of the winter was unusually cold. The measured maximum temperatures on 28th February, the last day of the meteorological winter, were the coldest on record in the Netherlands (Figure 1).
Sudden Stratospheric Warmings are events in the Northern Winter stratosphere which are often linked to outbreaks of cold Arctic air in Europe and North-America, like the one of February 2018. These Arctic air outbreaks are a consequence of a disturbed general circulation in the troposphere. An SSW might be responsible for a disturbed tropospheric circulation. But how is it possible that an event, which happens at such a long vertical distance, is still able to have influence on the troposphere?

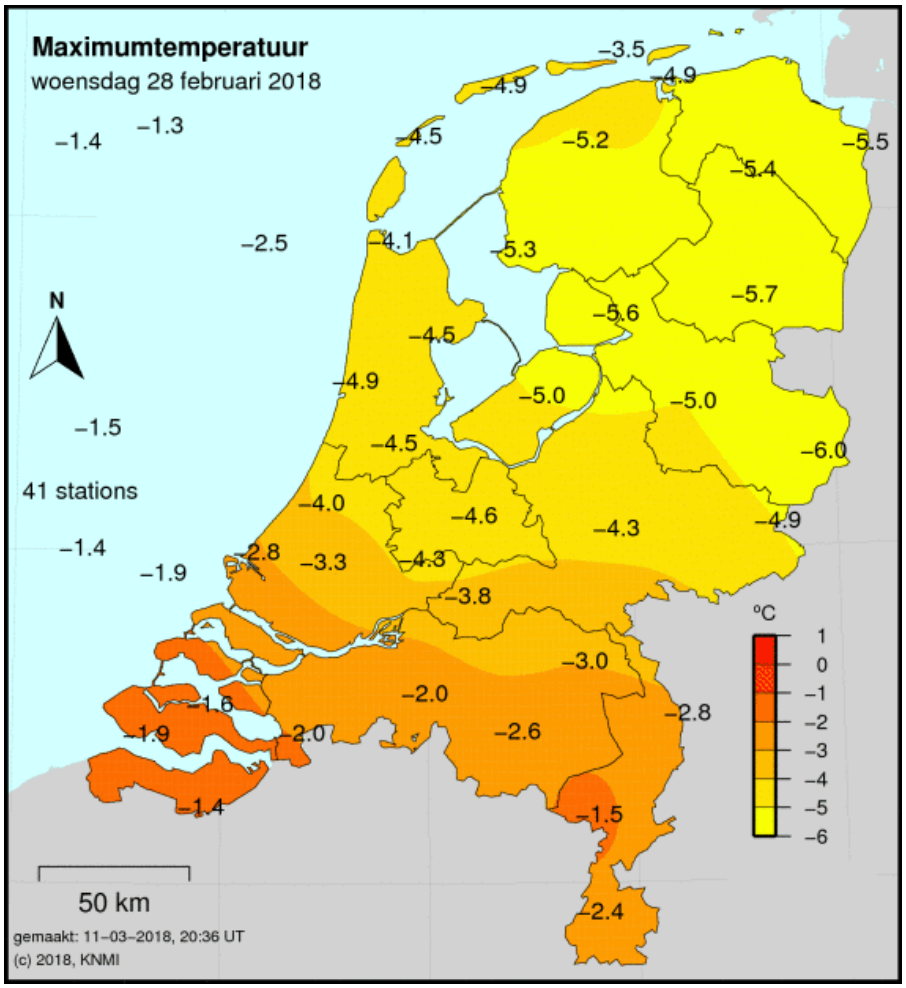

Figure 1: The maximum temperatures on 28 February 2018. It was never so cold in the Netherlands at the end of the Winter.

In this report, the influence of these events on the general tropospheric circulation is investigated. For this, we will use the so-called Deep Stratospheric Warming events (DSW), which are basically SSWs with some additional criteria regarding the vertical extent. The Potential Vorticity (PV) will be used as a quantity to explain the observed results in e.g. the pressure and wind deviations.

The main research goal is to understand what the mechanism is how an SSW high in the stratosphere can transport information downward in such a way that it significantly alters the general circulation. For this, the PV-θ view will be used, in which the potential temperature replaces the pressure as vertical coordinate. The main question is:

To which extent could the PV-θ view help to give a better explanation for the downward propagation of effects after a SSW and potentially affecting the NH general circulation in the troposphere?

Personal words and acknowledgement

I would like to thank my supervisors Aarnout van Delden and Michiel van Weele for guiding and supporting me in making this thesis. This topic is quite abstract and it was not always easy to work on it. Michiel provided me the opportunity to do this project at the KNMI. It was a good experience to share my research with other KNMI researchers and I learned a lot during this period.
I would also like to thank Lars van Galen, who also did a project on SSWs with Michiel. I had some interesting conversations with him where we shared our thoughts and ideas on each other work.

2 Theory

In this section, some important background and theoretical concepts are introduced which are needed to make a clear framework to describe the dynamics of an SSW. Firstly, the meaning and physical background of terms such as polar vortex and SSWs are explained. Secondly, the PV-θ view is introduced, which will form the theoretical framework to work in. Lastly, the relevance of the PV-θ view for SSWs and the downward effects is explained.

2.1 The polar vortex

2.1.1 Rossby waves

The polar vortex is a low-pressure system in the upper troposphere and stratosphere which is observed every winter half year, roughly between mid-autumn and spring. It is formed by the increasing thermal differences between the poles and equator; in autumn the poles cool down rapidly because of the longer nights (radiative cooling), causing increasing differences in temperature between the poles and equator in the stratosphere. During Spring, when the nights become shorter, the temperature differences between the poles and equator decrease and in the end, the polar vortex disappears. This happens at both the North Pole and South Pole. However, for the aim of this research, only the Northern polar vortex is of interest.

The polar vortex is not always stable. Vertically propagating Rossby waves, excited by the surface topography and thermal contrasts, can penetrate the polar vortex. From 'traditional' quasi-geostrophic theory, it can be derived that these waves can only propagate through the troposphere if the following conditions are satisfied:

$$0 < u - c < \frac{\beta}{K^2 + \gamma^2}, \tag{1}$$

where u is the zonal mean zonal wind, $K^2 = l^2 + k^2$, with k and l the wavenumbers in the x respectively y direction, β the Rossby parameter and $\gamma = 1/(2L_D)$ the inverse Rossby radius of deformation and c is the propagation speed of the wave. These conditions mean that Rossby waves can only propagate upwards if the zonal flow is eastward but not too strong (Figure 2). For stationary waves, c = 0. This condition is called the Charney-Drazin condition [1] [2]. Waves which do not satisfy this condition will reflect. Only waves which are long enough (and thus have a small wavenumber) are able to propagate through the polar vortex. Planetary waves with wavenumber 1 and 2 are favourable for the stratosphere [3].

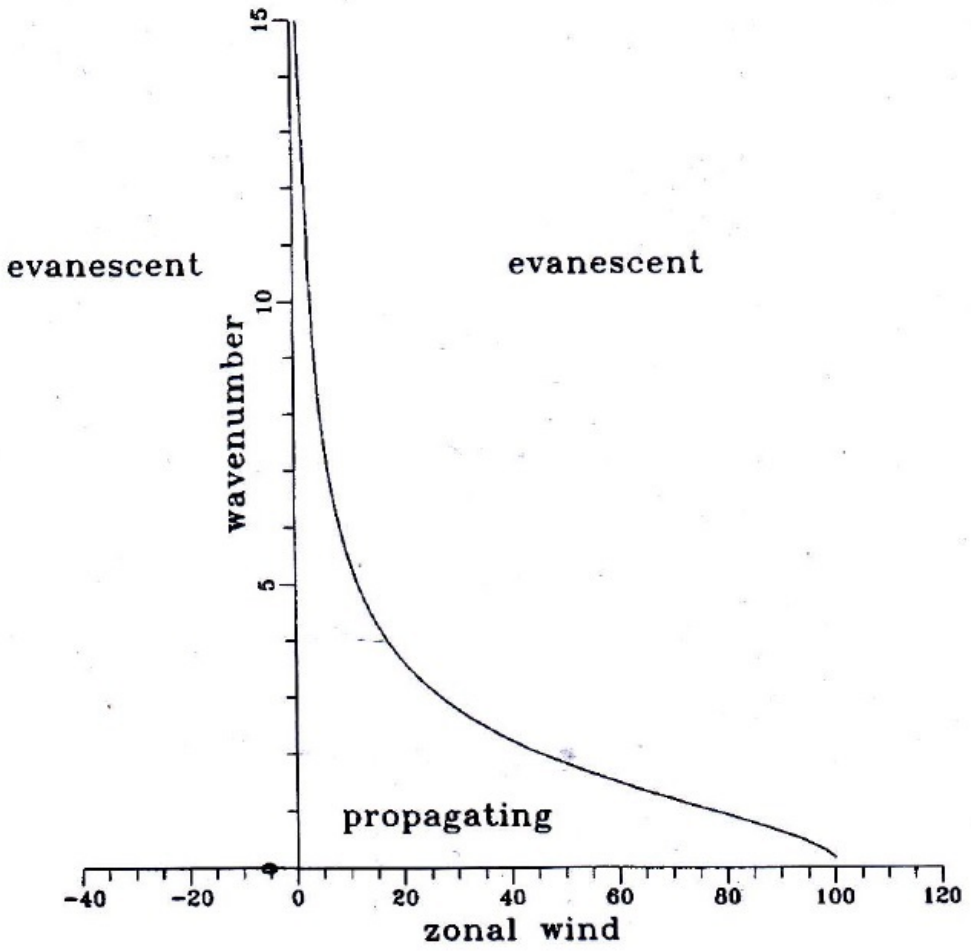

Figure 2: Graph which shows which planetary waves can propagate upwards and which planetary waves not. On the horizontal axis is the zonal wind speed given, on the vertical axis the total wavenumber K. Figure taken from [2].

The strength and amount of these waves depends on a quantity called the wave activity. The wave activity can be written in vectorial form, called the Eliassen-Palm flux. The meridional and vertical components of this vector denotes the meridional wave momentum flux and meridional wave heat flux, respectively. Waves which propagate upward and poleward transport heat and momentum. As they break or dissipate, exchange of momentum with the mean zonal flow occurs. This causes perturbations to the polar vortex.[4]

2.1.2 SSWs and DSWs

If the perturbations caused by the waves are strong enough, these may cause the vortex to displace or split into several parts. A rapid increase of temperature (30-50K within a few days) is observed during these events, which is explained by the adjustment to thermal wind balance. These events are called Sudden Stratospheric Warmings (SSW). SSWs can be divided into major SSWs, minor SSWs and final SSWs. The major SSW, according to the World Meteorological Organization (WMO), is defined as **"a reversal of the zonal mean zonal wind at a height of 10 hPa at a latitude of 60°N"**.
The minor SSW is defined as only the reversal of the polar meridional temperature gradient without a reversal of the zonal wind. The final SSW is the reversal of the zonal wind which remains easterly until the next autumn, when a new polar vortex forms [5]. For the purposes of these research, only SSWs of the major type are of importance since these events are expected to potentially have the largest influence on the general circulation in the lower stratosphere and troposphere.

One disadvantage of the current definition of a SSW is that it does not say anything about the vertical scale of the event. It does not provide any information about the downward evolution of information. The downward propagation of information may be of great importance for the influence on the circulation, incluidng that of the troposphere. Therefore, a new metric was developed which explicitly takes the downward extensions of the stratospheric perturbations into account: the Deep Stratospheric Warming (DSW)[7]. A DSW is defined as: **"a**

Table 1: SSWs and DSWs since 1979 based on ERA5

SSW date	DSW date	Type
22-02-1979	-	Split
29-02-1980	-	Displacement
04-03-1981	3-3-1981	Displacement
04-12-1981	-	Displacement
24-02-1984	12-03-1984	Displacement
01-01-1985	18-01-1985	Split
23-01-1987	09-02-1987	Displacement
08-12-1987	-	Split
14-03-1988	-	Split
21-02-1989	12-03-1989	Split
15-12-1998	-	Split
26-02-1999	04-03-1999	Split
20-03-2000	-	Displacement
11-02-2001	14-02-2001	Displacement
31-12-2001	-	Displacement
18-01-2003	-	Split
05-01-2004	28-01-2004	Displacement
21-01-2006	04-02-2006	Displacement
24-02-2007	-	Displacement
22-02-2008	-	Displacement
24-01-2009	28-01-2009	Split
09-02-2010	06-02-2010	Split
24-03-2010	-	Displacement
06-01-2013	18-01-2013	Split
12-02-2018	-	Split
01-01-2019	16-01-2019	Split

reversal of zonal mean zonal wind in a layer between 10-100 hPa for at least 5 days, averaged between 60-70 N. On at least 2 days, the layer thickness of the reversed zonal wind must be minimal 80 hPa". The requirements for a DSW are much stricter than for a SSW. These additional requirements enhance the chance that these events significantly affect the circulation in the lower stratosphere and troposphere .

A list of the noticeable official major SSW- and DSW events and the type of the event is given in Table 1. The data in Table 1 is derived using the ERA5 reanalysis data on pressure levels and compared to the dates found in [7], which was based on ERA Interim. The dates found using ERA5 are the same as in [7]. 1979, 1980 and 2019 are added in this table. The type of SSW is based on [8]. In total, since 1979 there were 26 SSWs and 17 DSWs; DSWs which were not preceded by an SSW are not included in Table 1 [1].

2.1.3 Stratospheric influence

In the period after a SSW, a period of abnormally cold winter weather is often seen in e.g. Europe and North-America [5]. In Western Europe, where mild westerly winds during winter are climatologically normal, this unusually cold weather is associated with high pressure systems at northern latitudes. These high pressure systems form a block: it blocks westerly wind to transport mild air to Europe, and it transports itself cold air, according to Buys-Ballot's law. High surface pressure over the polar cap together with low surface pressure at mid-latitudes corresponds to the negative phase of the Arctic Oscillation (AO). The AO is a climate variability parameter; it represents the winds circulating counterclockwise around 55°N. A positive phase corresponds to stronger winds and lower air pressure over the Arctic relative to lower latitudes and a negative phase to weaker winds and higher air pressure over the Arctic relative to lower latitudes. [2]. The North Atlantic Oscillation (NAO) is similar to the AO, but the NAO represents the difference in sea-level pressure between Iceland and the Azores. A positive phase of the NAO corresponds to low pressure above Iceland and high pressure above

[1] Table 1 shows only 13 DSWs instead of 17. The 4 other DSWs were not preceded by an SSW and started thus on lower levels in the stratosphere. The reason for not including those DSWs is that, for the later analysis in this thesis, events are selected which have their origin in the middle stratosphere (at 10 hPa).

[2] More precisely, the AO (index) is the leading EOF of the Northern Annular Mode (NAM), a more general climate variability parameter; see [9].

the Azores and a negative phase to high pressure above Iceland and low pressure above the Azores.

Commonly observed effects after a SSW are pressure increases at northern latitudes and changes in the circumpolar jet stream. One of the first papers on the effects due to downward propagation of an SSW was written by Baldwin and Dunkerton [9] [10]. They concluded that in the first 60 days after an SSW, the negative phase of the AO propagates downwards from the stratosphere to the troposphere. If the polar vortex is strong, there is an increased probability on a positive phase of the AO and NAO and if the polar vortex is weak, there is an increased probability on a negative AO and NAO. A negative phase of the AO and NAO is accompanied by pressure increases at northern latitudes.

The most observed changes in the circumpolar jet are weakening, meandering and equatorward displacement of the jet. Due to the equatorward shift, storm tracks have a more southerly position [11].

If SSWs are responsible for these disturbed circulations, a chain of events must happen to transport the perturbations high in the stratosphere to the troposphere. The effects of the SSW must propagate downward sufficiently enough to affect the circulation in the lower stratosphere and troposphere. A theory which tries to connect the downward propagation of perturbations to a change of the AO, is the 'mass-paradigm', introduced by Cai and Ren [6]. In this paradigm, it is described how 'warm' and 'cold' anomalies propagate poleward and downward initiate the transport of mass. The 'arrival' of anomalies at the stratospheric polar vortex coincides with the 'departure' of low tropospheric anomalies equatorward in the extratropics. A weaker mass circulation corresponds to a positive phase of the NAO and a stronger mass circulation to a negative phase of the NAO. The equatorward outflow of cold air mass is responsible for outbreaks of cold air.

2.2 Potential vorticity as a metric for SSWs

In dynamical meteorology (and geophysical fluid mechanics in general), potential vorticity (PV) is a commonly used quantity from which it is possible to deduce information of other meteorological quantities. In this subsection, the so-called PV-θ view and its usefulness is described.

2.2.1 The potential vorticity

There are multiple definitions of potential vorticity. For atmospheric sciences, the definition of PV by Ertel is widely used:

$$\mathcal{P} = -g(\zeta + f)\frac{\partial \theta}{\partial p}, \tag{2}$$

where potential temperature,

$$\theta = T(\frac{p_{ref}}{p})^{\frac{R}{c_p}}. \tag{3}$$

In these equations, $\mathcal{P}$ is the potential vorticity [3], θ is the potential temperature in Kelvin, ζ is the relative vorticity in s^{-1}, f is the planetary vorticity (which equals the Coriolis parameter $2\omega \sin \psi$) in s^{-1}, p the pressure in Pa and g the gravitational acceleration (9.81 ms^-2). T is the temperature in K, R = 287.058 J/kg/K the specific gas constant of air and c_p = 1005 J/kg/K the specific heat capacity of air. The unit of potential vorticity is thus $Km^2kg^{-1}s^{-1}$. A more convenient unit to express potential vorticity is the Potential Vorticity Unit (PVU): 1 PVU = $1 * 10^{-6} Km^2kg^{-1}$. The potential temperature increases with height. The PV definition can also be written in the more compact notation

$$\mathcal{P} = \frac{\eta}{\sigma}, \tag{4}$$

were $\eta = \zeta + f$ denotes the absolute vorticity, and $\sigma = -\frac{1}{g}\frac{\partial p}{\partial \theta}$ is the isentropic density parameter. It is important to note that the variables in this equations are expressed in isentropic coordinates, that is with the potential temperature as the vertical coordinate. This framework, in which the potential temperature is the vertical coordinate and the PV is the central metric, is called the PV-θ view. As will be shown later, this view

[3] In much literature about atmospheric dynamics, the term 'isentropic potential vorticity' (IPV) is used. In this thesis, 'potential vorticity' has the same meaning as isentropic potential vorticity

has very useful properties.
It is also possible to express the definition in terms of the static stability parameter[4] N^2:

$$\mathcal{P} = \frac{\theta}{\rho g}\eta N^2. \tag{5}$$

The 'equation of motion' in terms of potential vorticity (or simply the PV-equation) can be found by taking the total derivative of the definition of potential vorticity. The result is:

$$\frac{d\mathcal{P}}{dt} = \mathcal{P}\frac{\partial}{\partial\theta}\frac{d\theta}{dt} + \frac{1}{\sigma}\frac{\partial u}{\partial\theta}\frac{\partial}{\partial y}(\frac{d\theta}{dt}) - \frac{1}{\sigma}\frac{\partial v}{\partial\theta}\frac{\partial}{\partial x}(\frac{d\theta}{dt}) + \frac{1}{\sigma}(\frac{\partial F_y}{\partial x} - \frac{\partial F_x}{\partial y}), \tag{6}$$

where curvature terms are neglected. It turns out that under adiabatic ($d\theta/dt = 0$) and frictionless ($F_x, F_y = 0$) circumstances, potential vorticity is conserved on surfaces of constant potential temperature. This property makes potential vorticity a useful meteorological quantity. However, it might happen that diabatic effects become important and that the PV is not conserved. Neglecting friction and rewriting equation (6) leads to the following simplified PV-equation:

$$\frac{\partial\mathcal{P}}{\partial t} + u\frac{\partial\mathcal{P}}{\partial x} + v\frac{\partial\mathcal{P}}{\partial y} = -\frac{d\theta}{dt}\frac{\partial\mathcal{P}}{\partial\theta} + \mathcal{P}\frac{\partial}{\partial\theta}\frac{d\theta}{dt}. \tag{7}$$

The first term on the left-hand side is the local change of PV, the two other terms on the left-hand side are the advection terms. The first term on the right-hand side can be considered as diabatic advection of PV and the second term as the PV stretching-term. These two quantities contribute to the material change of PV on isentropes, and the generation of PV-anomalies, which will become important later. Note that both effects contain a total derivative of the potential temperature and are thus diabatic. From equation (7), it can be seen that in adiabatic circumstances, local changes in PV are fully attributed to local advection of PV.

In order to describe a dynamical system, we need to find an appropriate equation of motion. This will be done in the following subsections.

2.2.2 The flux of potential vorticity: isentropic mass and PVS flux

It may be useful to consider the fluxes of potential vorticity. In order to do that, the PV-equation (6) can be manipulated mathematically. It turns out that the PV-equation can be written in terms of the divergence of two quantities as follows:

$$\frac{\partial\mathcal{P}}{\partial t} = \frac{1}{\sigma}(\mathcal{P}\nabla\cdot\overline{I} - \nabla\cdot\overline{J}), \tag{8}$$

where $(I_x, I_y, I_\theta) = (u\sigma, v\sigma, \dot{\theta}\sigma)$ and $(J_x, J_y, J_\theta) = (u\sigma\mathcal{P} + \dot{\theta}\frac{\partial v}{\partial\theta}, v\sigma\mathcal{P} - \dot{\theta}\frac{\partial u}{\partial\theta}, 0)$. The vector $\overline{I}$ is the flux of isentropic mass (density) [5] and the vector $\overline{J}$ a quantity called Potential Vorticity Substance (PVS). To understand what PVS is, recall that the PV definition can be rewritten as $\mathcal{P} = \frac{\zeta+f}{\sigma} \equiv \frac{PVS}{\sigma}$. PVS is equal to the absolute vorticity: $PVS = \zeta + f$. So potential vorticity can be interpreted as a mixing ratio of a substance: the PVS. The PVS is thus the substance which can be transported (like a chemical tracer) [6]. The PV-equation in flux form (equation 8), is in fact a PVS-flux equation. The PV-equation can now be interpreted as follows: it describes the evolution of the mixing ratio of PV. The changes in potential vorticity are caused by convergence/divergence of isentropic mass flux and convergence/divergence of PVS flux. One striking thing is that the PVS-flux vector has no vertical component. In an isentropic coordinate system, this means that PVS cannot flow through an isentropic surface. This is called the impermeability theorem for PVS. The isentropic mass flux has a nonzero component if $\dot{\theta} \neq 0$ (i.e. in non-adiabatic circumstances). In conclusion, PV is a mixing ratio between PVS density and isentropic density [16].

According to equation (7), we may draw the following conclusion: downward vertical transport of perturbations in PV caused by an SSW, can take place via cross-isentropic downwelling of mass, or isentropic divergence of mass.

[4] Also known as the Brunt-Väisälä frequency. In this report, I will use the term 'static stability parameter' for this quantity

[5] Isentropic mass is the isentropic density integrated over the isentropic surface. However, in this report, both terms are used interchangeably. The physical consequences stay the same.

[6] One may notice that, unlike 'real' chemical tracers, the PV mixing ratio is not dimensionless. Also, PVS may be negative.

2.2.3 PV-invertibility: thermal wind principle in a PV-framework

It turns out that anomalies in the PV force a (zonal) wind anomaly. This can be proved by using the PV-invertibility equation. It turns out that the PV-invertibility equation is an expression of the thermal wind balance, expressed in terms of PV and potential temperature. The PV-invertibility equation is:

$$\frac{\partial}{\partial y}\left(\frac{\partial [u]}{\partial y} - \frac{[u]\tan\phi}{a}\right) + \frac{[\mathcal{P}]}{g}\frac{\partial}{\partial \theta}\left(f_{loc}\theta[\rho]\frac{\partial [u]}{\partial \theta}\right) = \frac{df}{dy} - [\sigma]\frac{\partial [\mathcal{P}]}{\partial y}, \tag{9}$$

where u is the zonal velocity, f_{loc} = f + (2[u] tan ϕ)/a the local Coriolis parameter corrected for curvature of the earth, σ the isentropic density, ρ the mass density, ϕ the latitude, θ the potential temperature, a the Earth's radius and g the gravitational acceleration. Quantities between square brackets [ ] denote the zonal mean of those quantities. A derivation of this equation can be found in [13] and appendix A; it follows roughly speaking from the hydrostatic balance and gradient wind balance in isentropic coordinates. This equation states the PV-invertibility principle: once the distribution of the potential vorticity is known, the other important meteorological quantities (such as u, v, T...) can be derived. What this equation makes useful is that it also states the thermal wind balance: it is the thermal wind balance in terms of the potential temperature and the zonal mean of the potential vorticity (gradients); see appendix A. This equation does not have an analytical solution, but it can be solved numerically. Numerical simulations shows that PV anomalies explain well the existence of multiple dynamical atmospheric phenomena; for example the stratospheric polar night jet owes its existence due to positive stratospheric PV anomaly in the NH-winter, see [13] for the exact details.

Disturbances of the potential vorticity induce a disturbance of the zonal mean state of the atmosphere. To show this, firstly start with decomposing the zonal mean of a dynamic variable X in a reference state X_{ref} and a anomaly X', for example the zonal wind. According to equation (9), an anomaly in the potential vorticity induces a cyclonic or anticyclonic motion, depending on the sign of the PV anomaly. To show this mathematically, a simplified solution to equation (9) will be derived [7]. The following assumptions are made: the curvature term is negligible ($\frac{[u]\tan\phi}{a} \ll \frac{\partial [u]}{\partial y}$), the Coriolis parameter is roughly constant, at northern latitudes ($f_{loc} \approx f_{ref} \approx 1 \times 10^{-4} s^{-1}$). Furthermore, $f_{loc}\theta[\rho]$ = constant and products of perturbations and their derivatives are small and thus negligible. Imposing these assumptions turns the PV-invertibility equation into:

$$\frac{\partial^2 [u]}{\partial y^2} + C\frac{\partial^2 [u]}{\partial \theta^2} = -\sigma_{ref}\frac{\partial \mathcal{P}'}{\partial y}, \tag{10}$$

with $C = \frac{f_{ref}\theta Z_{ref}[\rho]}{g}$ a constant. This equation can be solved by assuming two solutions of the form $[u] = U(\theta)\sin\left(\frac{2\pi(y_{NP}-y)}{L}\right)$ and $\mathcal{P}' = \mathscr{P}'(\theta)\cos\left(\frac{2\pi(y_{NP}-y)}{L}\right)$, with y_{NP} the distance from the equator to the North Pole and L some horizontal scale length to nondimensionalize the sine and cosine terms. Assuming that $|y_{NP} - y| \leq L/2$ and that the PV-anomaly is located at some discrete 'height' θ_0, the solution of $\mathcal{P}'$ is as follows:

$$\mathcal{P}' = \mathcal{P}'_{max}\delta(\theta - \theta_0)\cos\left(\frac{2\pi(y_{NP}-y)}{L}\right), \tag{11}$$

with $\delta(\theta - \theta_0)$ being the Dirac-Delta function. Plugging the test solutions (note that the right hand side becomes zero for $\theta \neq \theta_0$) into equation (10) gives as solution for $U(\theta)$:

$$U(\theta) = D_1 e^{\frac{2\pi(\theta-\theta_0)}{L\sqrt{C}}} + D_2 e^{-\frac{2\pi(\theta-\theta_0)}{L\sqrt{C}}}. \tag{12}$$

At first sight, this function does not have a potential vorticity anomaly dependence, but remember that a PV-anomaly is placed at $\theta = \theta_0$. Requiring that far from the PV-anomaly the wind goes to zero (we do not want infinite wind speeds), we can set D_1 to zero. By requiring a maximum wind velocity at $\theta = \theta_0$, D_2 can be set to u_{max}. The final solution of u is then:

$$u(y,\theta) = u_{max}e^{-\frac{2\pi(\theta-\theta_0)}{L\sqrt{C}}}\sin\left(\frac{2\pi(y_{NP}-y)}{L}\right). \tag{13}$$

[7] This derivation closely follows [12]

From this equation, it becomes clear that a maximum wind velocity coincides with a maximum PV-anomaly. This principle is explained in Figure (3):

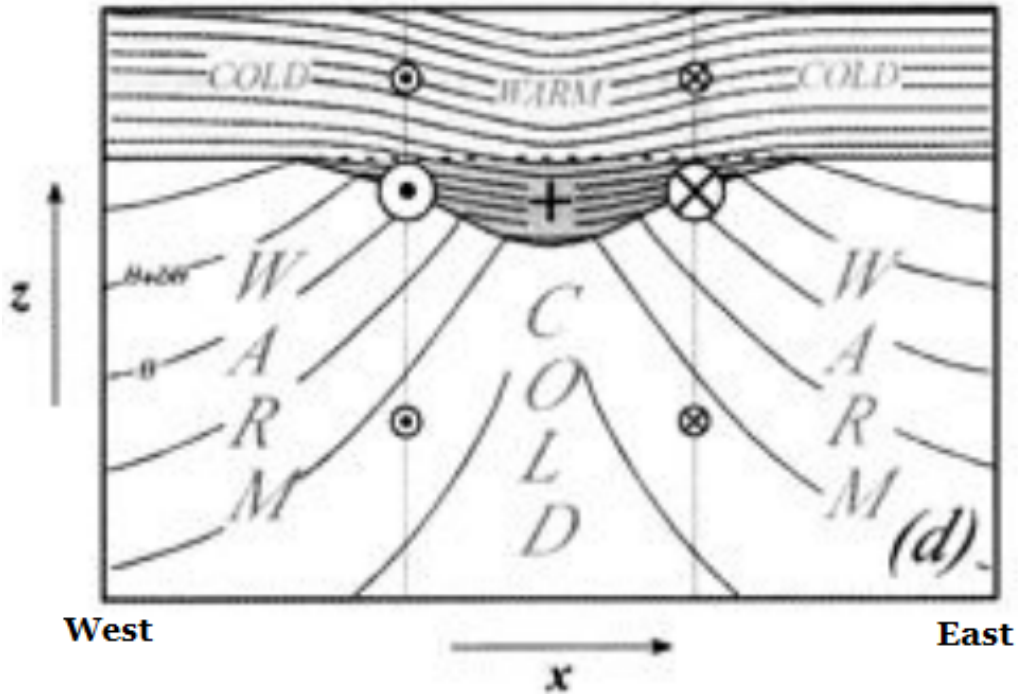

Figure 3: Schematic representation of a positive PV-anomaly (shaded). The black thick line denotes the tropopause, which is defined as the 1.5 reference PVU line (figure from [14]).

The dynamical tropopause, which is often defined as the 1.5 PVU reference potential vorticity plane, seperates tropospheric air from stratospheric air. When the tropopause folds, stratospheric air can intrude the tropospheric air which plays an important role in tropospheric cyclogenesis. Note that, since θ increases with height (and thus decreases with p!), that from the definition of potential vorticity follows that the PV also increases with height. A positive anomaly is created when a line of constant PV (in this case the tropopause) bulges downward locally. Due to a positive PV-anomaly, isentropes below the anomaly are forced to bow towards the anomaly. The air is here locally colder than the direct surroundings. The isentropes above the anomaly bulges towards the anomaly. Here, the air is locally warmer than the direct surroundings. Due to thermal wind balance ($\frac{\partial T}{\partial x} \sim \frac{\partial v_y}{\partial z}$), at the left edge of the anomaly, an outward wind (out of the paper) is being induced. At the right edge, the PV anomaly induces an inward (into the paper) wind. The result of a positive PV-anomaly is thus a cyclonic wind circulation. According to the thermal wind principle, the strongest wind shear is found at the biggest horizontal temperature gradient. In case of a negative PV anomaly, the reverse happens: the tropopause bulges upwards and creates a negative PV-anomaly. Isentropes below the anomaly bend away from it, as well as the isentropes above the anomaly. Below the anomaly it is locally warmer than the surroundings and above the anomaly it is locally cooler than the surroundings; at the left edge of the anomaly, an inward wind is being induced and at the right edge an outward wind; the result is an anticyclonic wind circulation. Kleinschmidt interpreted PV-anomalies as charges which induces a wind field as electric charges induce an electric field.[15].

The invertibility principle has also other physical effects. Below the positive anomaly, isentropes are raised indicating that the air mass cools down and becomes heavier. This depresses the isobars below the anomaly. Above the positive PV-anomaly, where the isentropes are lowered, the air becomes warmer and less dense and as a consequence the isobars are raised above the PV-anomaly. One can apply the same arguments to show that for a negative PV-anomaly the isobars raises below the anomaly and depressed above the anomaly. Also note that the isentropes above the tropopause are more closely packed than below. As can be immediately seen from the definition of isentropic density, it implies that the stratospheric air is more stable than tropospheric air. Convection is mostly suppressed, so vertical mixing does not happen a lot. From the definition of potential vorticity, it can be easily seen that a positive PV-anomaly results from both a positive anomaly in the relative vorticity and a negative anomaly in the isentropic density (equation 4). [**?**]. The reverse holds naturally for a negative anomaly. How the PV-anomalies are calculated will be explained in section 3.2

2.2.4 The Rossby scale height

From equation (13), it follows that the zonal wind adjusts to a certain PV-anomaly over some vertical range. This vertical range is:

$$\Delta\theta = \frac{L\sqrt{C}}{2\pi} = \sqrt{\frac{L^2 f_{ref}\theta\mathcal{P}_{ref}\rho}{4\pi^2 g}}. \tag{14}$$

This quantity is called the Rossby scale height. It is the vertical range over which the zonal wind speed has fallen of by a factor 1/e. This quantity can thus be considered as the response range of a PV anomaly. The Rossby scale height can also be expressed in terms of the static stability parameter, $N = \sqrt{\frac{g}{\theta}\frac{\Delta z}{\Delta\theta}}$ and the inertial frequency, $F = \sqrt{f(f+\zeta)}$:

$$\Delta\theta = \frac{L}{2\pi}\frac{\theta}{g}FN. \tag{15}$$

Converted into meters, this equation takes the form:

$$\Delta z = \frac{L}{2\pi}\frac{F}{N}, \tag{16}$$

where N≥0 and F≥0 [8], see appendix B for a derivation. The horizontal length scale L can now be set to the size of the polar vortex. A reasonable estimation of the diameter of the stratospheric polar vortex is 6000 km. Assuming that the edge of the vortex is located at 65 $^\circ N$, a simple geometric estimation gives a diameter of the polar vortex of approximately 5600 km [9]. An estimation for the stratosperic polar vortex (L = 6000 km, $\theta = 850K$, $\mathcal{P}_{ref} \approx 350PVU = 350 * 10^{-6} Km^2 kg^{-1} s^{-1}$, $\rho \approx 0.02 kg/m^3$, $N \approx 10^{-2} s^{-1}$ and $F \approx 10^{-4} s^{-1}$, gives $\Delta\theta \approx 225$ K and $\Delta z \approx 9.5$ km.

To conclude this section, the following summarizing statements can be made:

- **The PV-θ view is a useful framework to work in because of the conservation of PV, the impermeability of isentropes to PVS and the invertibility principle.**
- **The PV-evolution equation tells how PV-anomalies arise and diminish.**
- **The PV-inversion equation tells how PV-anomalies can alter the circulation.**
- **The Rossby scale height is the vertical range of a PV anomaly, in which air parcels can be influenced by that anomaly.**

[8] One may notice that negative values of F^2 and N^2, and thus imaginary values of F and N, are physically perfectly allowed. But this would mean that $\Delta\theta$ and Δz may also become imaginary, which does not make sense physically. However, since the PV-invertibility equation assumes both hydrostatic balance and thermal wind balance, the Rossby scale height only applies for balanced systems. In other words, in the $PV-\theta$ view, N $\geq$ 0 and F $\geq$0.

[9] Take R = 6371 km as the earths radius and a the arc length from 65 °N to the North Pole. The length of the arc and thus the distance to the pole is a $\approx R\theta = 6371 * ((90-65) * \frac{\pi}{180}) \approx 5600km$

3 Methods

An SSW can be considered as a big disturbance in the stratosphere with a certain vertical extent. These disturbance change the PV distribution, which leads to a PV anomaly over the pole. These PV anomalies affect the troposphere if the Rossby height is big enough. The physics of the tropospheric influence is contained in the PV-invertibility principle: it is adjustment of the zonal mean state to thermal wind balance. To investigate the effects of SSWs on the troposphere, it is useful to consider the evolution of PV anomalies and the factors which cause the PV-anomalies to change. In this section, it will be explained how that is done. These methods consider the determination of the PV anomalies, the meridional fluxes of isentropic mass and PVS and the Rossby scale height and static stability before and after a SSW.

3.1 The case studies

Since there are only 17 [10] SSW events since 1979 which fulfill the DSW conditions, it is hard to make a reliable statistical analysis. It may be therefore more useful to select some cases and analyze these cases in detail. The selected cases are the DSW events of 1985, 2009, 2013 and 2019 and one case (February 2018) which did not satisfy the DSW criteria but had nevertheless a big impact on the troposphere. For these case studies, the ERA-5 reanalysis data is used. The ERA-5 data runs from 1979 to May 2019 (at the time that this report is written). These data have 137 vertical layers. These data are centralized around the Central Date of the DSW, that is, the first day on which the DSW criteria are satisfied. Day 0 corresponds to the Central Date of the DSW. A period of 40 days is considered (with exception of the DSW of 1985, for which a 60-day period is considered due to the long time between the SSW and DSW that year), which should be long enough to obtain the effects of the event. The date on which the SSW criteria are satisfied are also included. The state of the polar vortex 15 days before and after the SSW is also considered, as well as the state of the tropospheric circulation. The initial state of the atmosphere may have a significant influence on the ultimate effects of an SSW has on the circulation.

For every case, altitude-time (θ, t)) diagrams of the zonal mean zonal wind, potential vorticity anomalies, isentropic mass flux and PVS flux are provided, as well as the evolution of the pressure planes. The zonal means of those quantities are taken. For the pressure and the PV anomaly, a mean over the Polar Cap, which is averaged between 65-89 $^\circ$ N is taken[11]. The zonal wind, isentropic mass and PVS fluxes are evaluated at $65°N$. This latitude represents the edge of the Polar Cap. To get some insight into changes to the mass circulation, every case has a plot of the cumulative mass and PVS fluxes and their eddy and mean circulation components. At last, for every case the evolution of the static stability parameter N^2 and Rossby scale height $\Delta\theta$ is given, which provides some information on the vertical reach of the PV anomalies.

All the calculations and figures are made in the programming language Python.

3.2 Determination of PV anomalies

In order to determine the anomalies of the potential vorticity, we need to define a reference state. We start with determining the reference state of the isentropic density σ. It will turn out that a latitudinal mean of the isentropic density is a good reference state:

$$\sigma = \frac{\int \sigma \cos\phi d\phi}{\int \cos\phi d\phi} \equiv \sigma_{ref}(\theta, t). \tag{17}$$

The reference state of the PV is then given by:

$$\mathcal{P}_{ref} = \frac{f}{\sigma_{ref}} \equiv \mathcal{P}_{ref}(\theta, \phi, t). \tag{18}$$

So the reference state of the potential vorticity depends on the location and time. The anomalies are then obtained by:

$$\mathcal{P}' = [\mathcal{P}] - \mathcal{P}_{ref}. \tag{19}$$

This choice of reference state has also a physical implication. If we let $[\sigma] = \sigma_{ref}$ and $[\mathcal{P}] = \mathcal{P}_{ref}$, the PV-invertibility equation will make the right-hand side zero. There is no forcing and the only trivial solution

[10] As mentioned earlier, 4 DSWs are not included in Table 1 since they were not preceded by an SSW.

[11] At a latitude of 90°N, the reanalysis data of the wind is incorrect (see `https://confluence.ecmwf.int/pages/viewpage.action?pageId=129134800`). That is why the mean between 65-89 is taken for these studies

is then [u] = 0 if the boundary conditions are homogeneous. What this physically means is that in absence of PV-anomalies, the atmosphere is in a state of rest. So stated in other words: PV-anomalies measure how much the atmosphere is deviated from its state of rest (if the boundary conditions are homogeneous).

3.3 The total flux of mass and PVS and the relation with zonal wind

In order to get some insight into the incoming and outgoing mass- and PVS fluxes by meridional circulations, the total meridional flux in a layer can be determined by:

$$\Delta F_X(t) = \int_{t_0}^{t} \int_{\theta_0}^{\theta_1} [vX] d\theta' dt', \tag{20}$$

where 'X' can be either isentropic mass or PVS. It is a vertically integrated function of time, which represents the accumulated flux integrated over a vertical layer in time. θ_0 is the lower boundary of the vertical layer and θ_1 the upper boundary. t_0 denotes the time at the beginning of the period and t is the current time. This integral is performed for the mid-stratosphere (600-850K) and lower stratosphere (395-530K).

Both fluxes can be decomposed into two parts:

$$[vX] = [v][X] + [v * X*], \tag{21}$$

The first term of the right hand side denotes the flux due to the mean circulation and the second term the fluxes due to eddies. It turns out that the PVS flux (especially the eddy PVS flux) acts as a zonal external force. More precisely, a poleward PVS flux exerts an eastward zonal force which accelerates the eastward flow. An equatorward PVS flux decelerates the zonal flow. This can be shown mathematically as follows. Consider a disk at some latitude with radius $R\cos\phi$. The mean PVS (PVS and absolute vorticity are equivalent) in that disk can be calculated as:

$$\overline{PVS} = \frac{2\pi[u]R\cos\phi}{\pi(R\cos\phi)^2}, \tag{22}$$

where the term in the numerator comes from Kelvins circulation theorem (the mean PVS is thus the circulation per unit area). A change of the mean PVS in the disk can be written as:

$$\pi(R\cos\phi)^2 \Delta\overline{PVS} = (2\pi R\cos\phi)\Delta F \tag{23}$$

where ΔF is the PVS flux along the edge of the disk. Combining (22) and (23) gives:

$$\Delta F = \Delta[u],$$

which demonstrates that a poleward (positive) PVS flux accelerates the zonal wind and that an equatorward (negative) PVS flux decelerates the zonal wind. This force coming from the equatorward PVS flux is called planetary wave drag [20]. The polar jet at $60°N$ is mainly driven by eddies: that is why the polar jet is also called the eddy-driven jet.

3.4 Projection

In order to get a good spatial view of the physical quantities (temperature, zonal wind and geopotential height) around the pole, the distortions need to be minimized. A way to achieve this is to make use of an orthographic projection. If we project right on the North Pole ($\phi = 90°$, $\lambda = 0°$), the right coordinate transformation becomes [21]:

$$\begin{aligned} x &= +R\cos\phi\sin\lambda \\ y &= -R\cos\phi\cos\lambda, \end{aligned}$$

with a corresponding line element:

$$ds^2 = R^2 \sin^2 \phi d\phi^2 + R^2 \cos^2 \phi d\lambda^2.$$

R is the radius of the projection sphere and is constant; it is the distance such that the projection catches the whole Northern Hemisphere, i.e. the radius of the Earth. This line element is invariant on distance between circles parallel to the projection plane [12] . The invariance of the line element means that around the North Pole, the distortions are minimal. Around the edges of the sphere, the distortions get more significant, but since the point of focus is around the North Pole, this is not a big issue. This projection is contained in the cartopy package of Python and will be used to project spatial data. This is done on a grid of 1*1 degrees.

3.5 Other information

The size of the polar vortex is quite hard to estimate due to its variability in shape and diameter. To tackle this issue, we assume a circular vortex with the edge at $\phi = 65°N$. As calculated in the previous section, the vortex has then a diameter of approximately 5600 km; we round this up to 6000 km. A uncertainty marge of 10 % is included in order to incorporate the uncertainty of the polar vortex size.

The density varies with height in the stratosphere and troposphere. For simplicity, the values according to the U.S. Standard Atmosphere 1976 are taken, in which the density decreases exponentially with height [22]. For example, at 10 hPa, the density is roughly 0.017 kg/m^3 in this model.

[12] This can be mathematically shown by computing the Killing vectors of symmetry, which are for this coordinate transformation $\mathbf{K}$ = (0,1) and $\mathbf{R} = (\sin\phi, \cos\phi)$. Details can be found in [21] or other any other textbook on cartography calculus

4 Results of the case studies

In this section, five cases of SSW and DSWs and the consequences on the tropospheric circulation are explored. Each case is divided into four parts. These cases ar the events of 1985, 2009, 2013, 2018 and 2019. In the first part, the state of the polar vortex 15 days before and after the date of the SSW is analyzed. This is done by calculating and plotting the geopotential height and the temperature, both at 10 hPa. In the second part, the tropospheric circulation 15 days before and after the SSW date is analyzed by plotting the geopotential height and zonal wind, both at 300 hPa. By comparing the changes in the tropospheric pattern, it can be deduced how strong the tropospheric reaction of the SSW was. In the third part, the vertical evolution of PV anomalies, zonal wind, isentropic mass flux, PVS flux and pressure is analyzed as well as the accumulative integrated mass and PVS flux in the mid stratosphere (600-850K) and lower stratosphere/upper troposphere (395-530K). In appendix C, tables with the values of the mass and PVS flux on each isentropic level available are given. In part four, the Rossby scale height and the static stability parameter for each case is calculated to measure the vertical range of influence.

4.1 1985

The SSW of 1985 took place officially on 1 January 1985, and the DSW followed on 18 January 1985. The SSW resulted in a split of the polar vortex.

1. The polar vortex state

In Figure 4, two snapshots of the polar vortex at 10 hPa 15 days before and after the SSW date are shown.

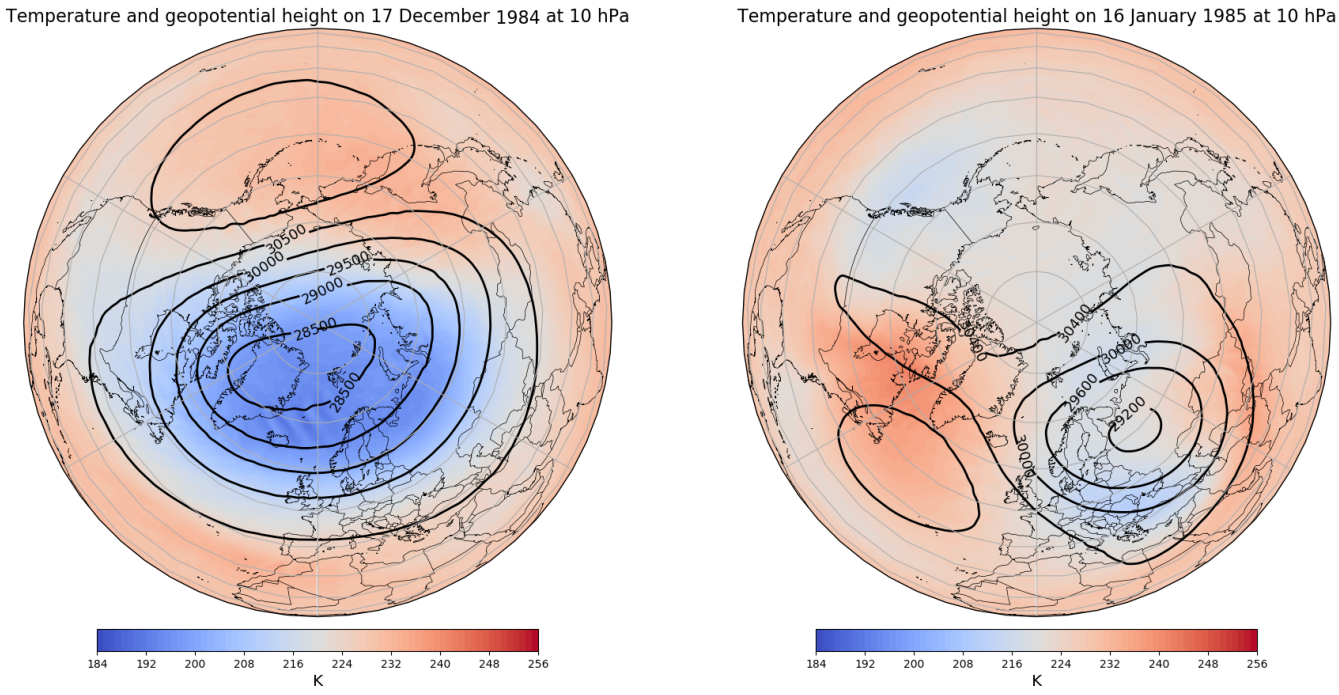

Figure 4: The polar vortex 15 days before (left) and 15 days after (right) the SSW on 1 January 1985. The black contours denote the geopotential height in meters. The blue and red colours denote the temperature in Kelvin.

On 17 December 1984, the polar vortex roughly spans from the East-coast of North-America to Siberia, with its core above the northern Atlantic Ocean, between Greenland and Svalbard. The vortex is relatively elongated and has some ripples. A strong polar vortex is characterized by a axisymmetric smooth shape, like a circle. This vortex is not very axisymmetric, an indication that the vortex was already disturbed by waves 15 days before the SSW. On January 16, Figure 4 right panel, a displaced cold vortex is visible above Russia. What happened is that the original vortex broke apart into two daughter vortices and merged again to one vortex above Russia. The horizontal temperature gradients are reduced, since the coldest air is less cold compared to that of the vortex on 17 December 1984.

2. Tropospheric reaction

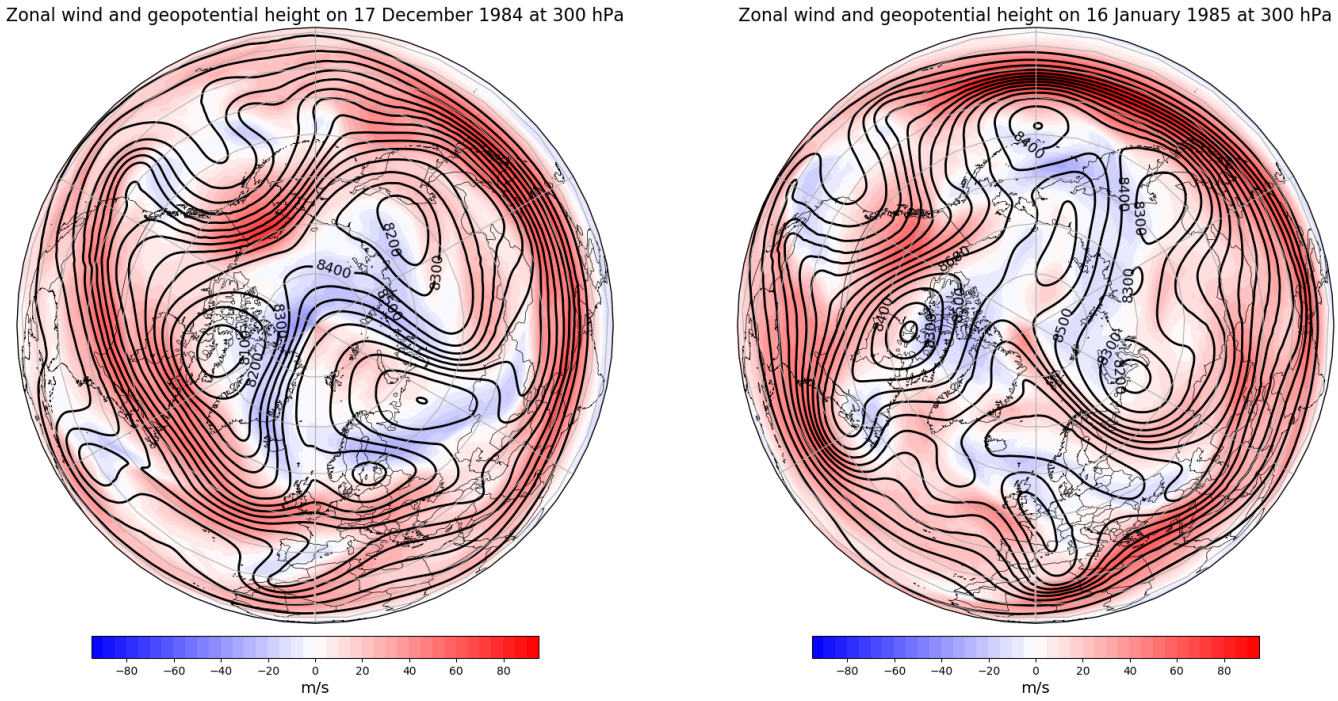

Figure 5: Maps of the zonal mean zonal wind and geopotential height at 300 hPa 15 days before (left) and 15 days after (right) the SSW of January 1985. The black contours represent the geopotential height. The red colour denotes positive (eastward) zonal wind and a blue colour negative (westward) zonal wind.

In Figure 5, two maps are shown of the zonal wind and geopotential height at a height of 300 hPa. On 17 December 1984 (left panel), there was a strong jet flowing above midlatitudes, but there were also some areas with an easterly (negative zonal) wind. Also striking are the low geopotential heights above Greenland and high geopotential heights above Russia, indicating low pressure above Greenland and high pressure above Russia; one can say that the atmosphere is semi blocked.
On 16 January 1985 (right panel), 15 days after the SSW and 2 days before the DSW, the jet has shifted significantly equatorwards with some meanders. Easterly winds are found over large parts of Europe. Areas of high geopotential heights and pressure are visible above Greenland and Scandinavia, while areas of low geopotential heights and low pressure are found above Russia and Canada. This is an example of a clearly blocked atmosphere above Europe, characterized by a negative NAO and AO.

3. The SSW-DSW event

In Figure 6, the vertical time evolution of the zonal mean zonal wind at 65°N and of the zonal mean pressure, potential vorticity and static stability averaged between 65-89°N is plotted. In Figure 7a, the pressure and potential vorticity are also plotted but now with the isentropic mass flux at 65°N instead of the zonal wind and likewise in Figure 7b, with the PVS flux at 65°N plotted.

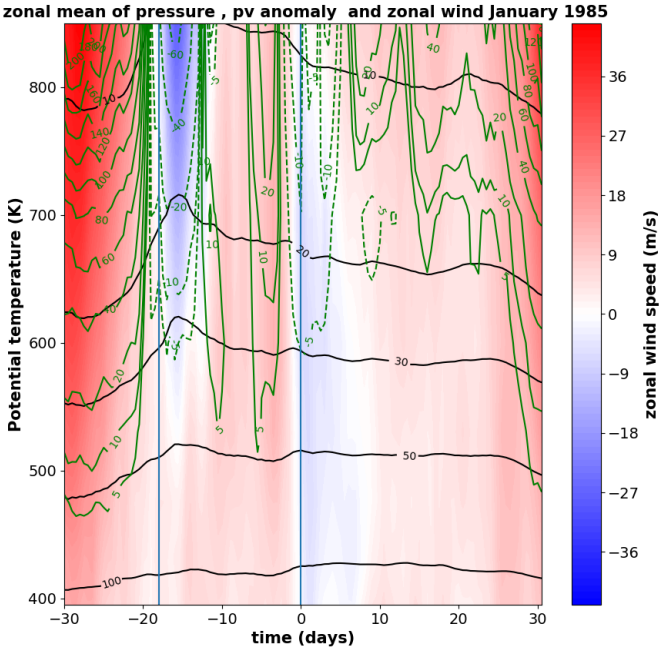

Figure 6: (θ-t)-plot of December 1984/January 1985. The horizontal axis denotes the time in days, where day 0 corresponds to the day of the DSW. The vertical axis denotes the potential temperature level. The black contour lines represent the zonal mean pressure in hPa and the green contour lines the zonal mean of potential vorticity anomalies in PVU; dashed contour lines denote negative values. The blue colour represents a negative zonal mean zonal wind speed, the red colour represents a positive zonal mean zonal wind speed. The zonal mean zonal wind speed is calculated at 65°N, while the zonal mean pressure and PV anomaly are averaged between 65-89 °N. The first vertical blue line corresponds to the SSW date (1 January 1985), the second blue line to the DSW date (18 January 1985).

Looking at Figure 6, the following features can be observed. The zonal wind is strongly positive before the SSW date but suddenly becomes negative above a level of 600K for some days before it gets positive again. Around the DSW date, the zonal mean zonal wind is slightly negative but becomes positive shortly after the DSW date.
The isobars start to increase in height before the SSW, where the most significant response can be seen in the mid stratosphere. This raise of the isobars indicates a higher pressure. The raise of isobars in the lower parts of the stratosphere lags some days compared to that in the mid stratosphere and shrinks in amplitude. Some days after the SSW date, the isobars start to decrease in height. This decrease of pressure continues till the end of the period.
Before the SSW, a very positive PV anomaly of more than 200 PVU in the mid stratosphere can be observed. Directly after the SSW date, the PV-anomaly suddenly drops towards negative values, whereas it becomes positive about 6 days after the SSW. At the CD, the PV-anomaly becomes negative again for a short time. After this time, the PV-anomaly turns back to positive values. It keeps on growing till the end of the period. The largest (positive and negative) PV-anomalies are seen high in the stratosphere. The PV-anomalies reach a depth of about 500K (50 hPa).

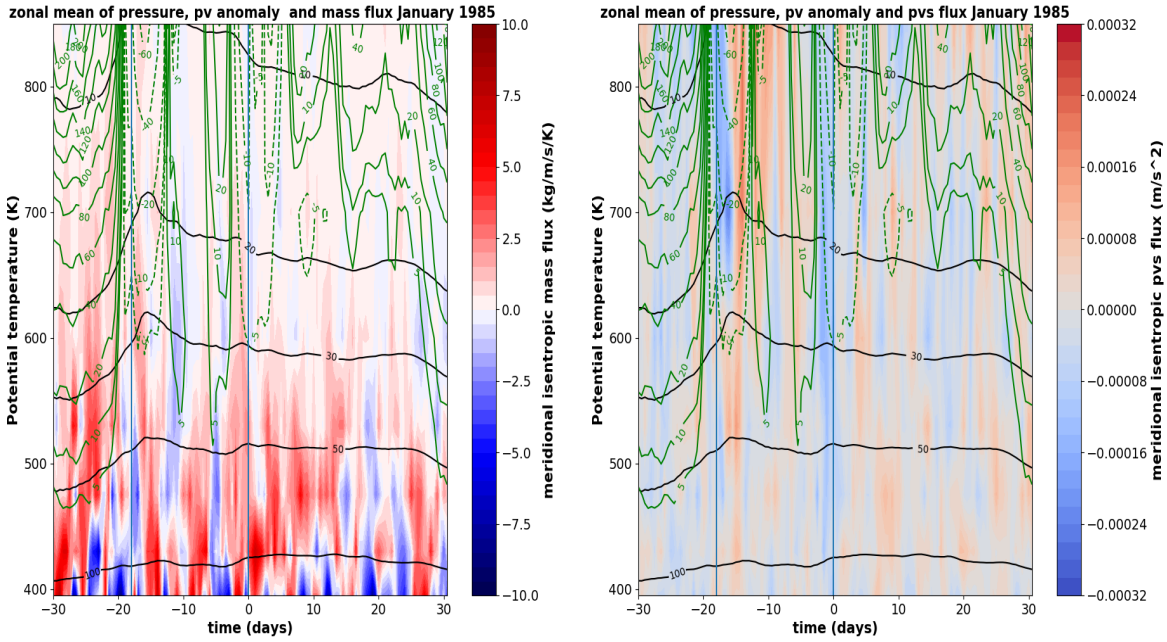

(a) Isentropic mass flux

(b) PVS flux

Figure 7: As Figure 6, but now with the zonal mean isentropic mass flux (left panel) in kg/m/s/K and zonal mean PVS flux (right panel) in m/s^2 instead of the zonal wind. Both fluxes are calculated at 65°N.

In Figure 7a, the isentropic mass flux is shown with again the isobars and PV-anomalies. The more significant mass fluxes are clearly in the lower part of the stratosphere, below roughly 600K (25 hPa). The signal fluctuates, but it seems that after the SSW, the mass flux in the lower parts of the stratosphere tends to become polewards while in the upper part of the stratosphere it becomes equatorwards.
In Figure 7b, the isentropic PVS flux is shown. Before the SSW, it is equatorward in the higher stratosphere, after the SSW is becomes shortly positive and then turns back into negative values. The signal also fluctuates but it is less compared to the mass flux. A band of positive PVS fluxes around 50 hPa can be seen.

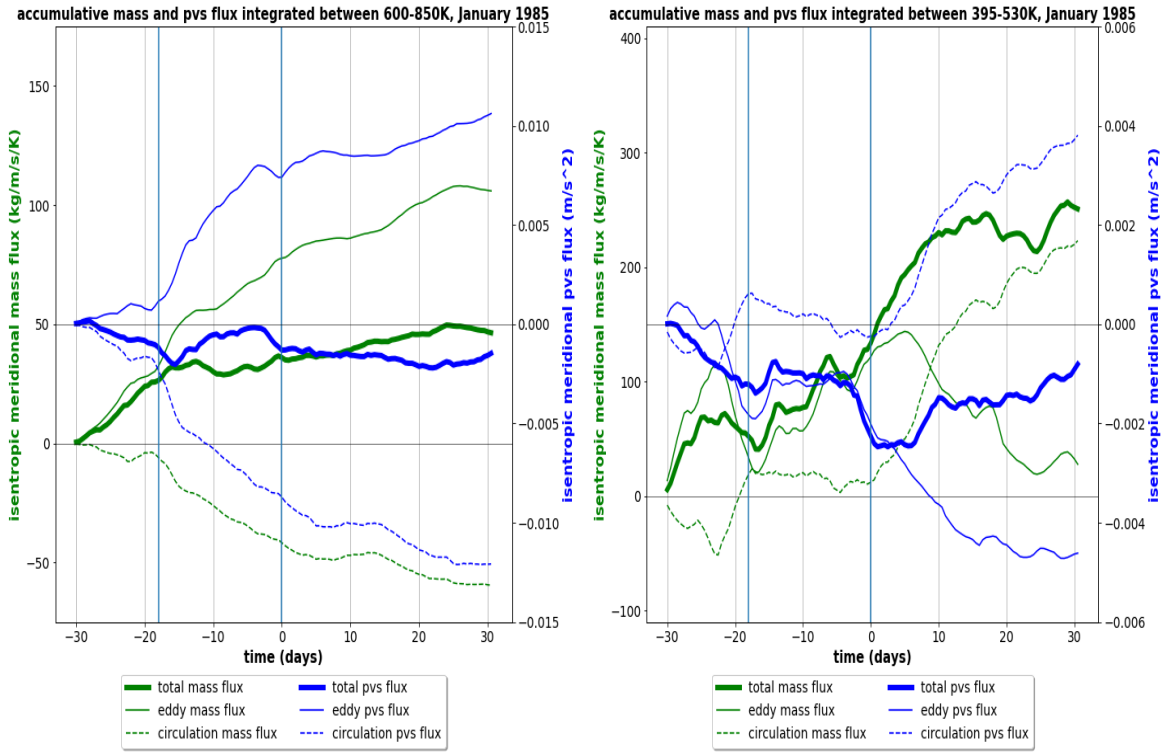

(a) 600-850K

(b) 395-530K

Figure 8: The accumulated isentropic mass and PVS flux of January 1985. (a) shows the accumulative fluxes integrated in a layer between 600 and 850K, (b) the accumulative fluxes integrated in a layer between 395-530K. Both fluxes are calculated at 65°N. The thick green lines represent the total mass fluxes and the thick blue lines the total PVS fluxes, which are both decomposed in fluxes due to eddies (solid thin) and the mean circulation (dashed)

Figure 8a shows the accumulative mass and PVS fluxes and the eddy and mean circulation components of those fluxes integrated over a layer between 600-850K. It can be seen that before the SSW, the total [13] mass flux (green curve) increases while the total PVS (blue curve) flux decreases. For both mass and PVS flux, the mean circulation flux increases while the eddy circulation flux decreases; it follows almost an anticorrelated relation. During this phase, the eddy mass flux is clearly dominant over the mean circulation; the reverse holds for the eddy and mean circulation PVS flux. After the SSW, the total mass flux increases slightly while the PVS flux increases shortly and then decreases. The changes are small. At the end of the period, the total accumulative mass flux is positive, the total accumulation of PVS flux is then negative. Both changes in eddy and mean circulation components are small in this period.
Figure 8b shows the same, but then integrated over a layer between 395-530K. Just before the CD, the accumulative total mass flux increases significantly while the accumulative total PVS flux drops quickly. The eddy mass flux decreases after the CD while the mean circulation mass flux increases significantly. The same holds for the eddy and mean circulation PVS flux. In the end, the total accumulative mass flux is positive and the total accumulative PVS flux is negative.

4. Rossby height and static stability

Initially at the 850K level, both the Rossby height and static stability are high but drop quickly some days before the SSW. They reach their minimum shortly after the SSW. For the Rossby height, this minimum lies between 230 and 280K and for the stability around $6 * 10^{-4} s^{-2}$. Both parameters increase gradually after their minimum.
At 500K, both the Rossby height and static stability decrease as well initially. After the CD, the static stability and Rossby height reaches their lowest values during some days: 115-140K and $3.5 * 10^{-4} s^{-2}$, respectively.

[13] With 'total', the sum of the eddy and mean circulation flux is meant.

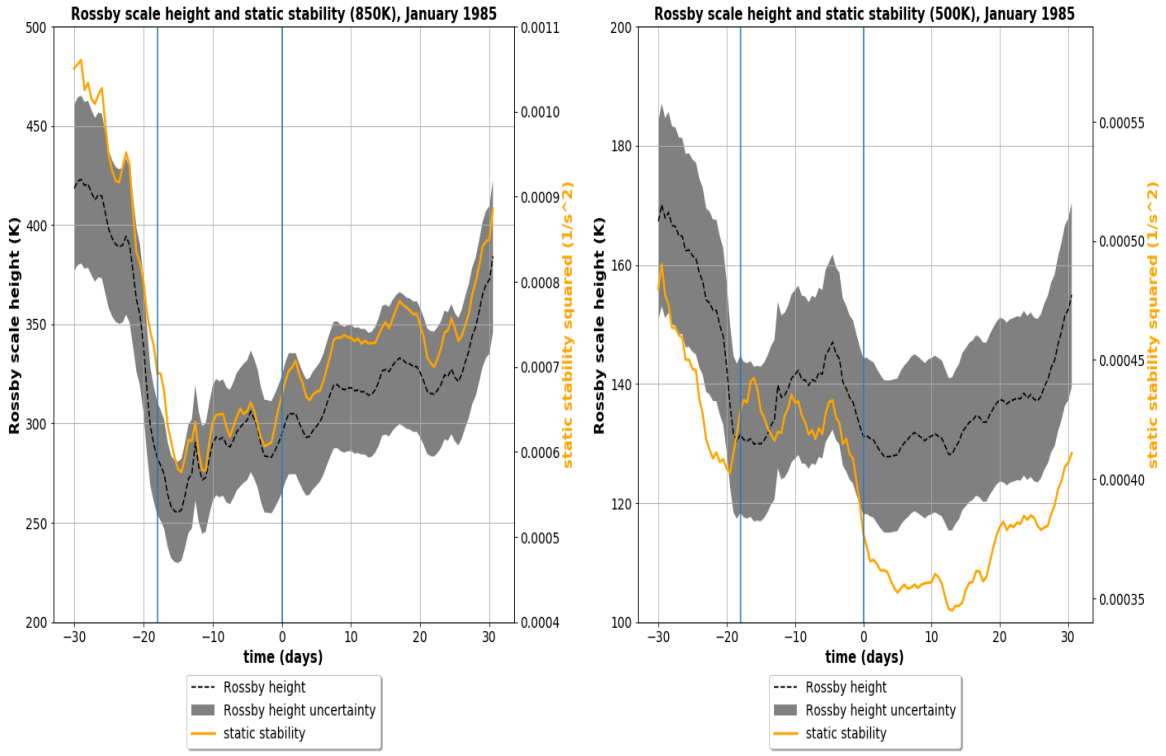

(a) 850K

(b) 500K

Figure 9: Rossby height and the zonal mean static stability of January 1985 at 850K (left) and 500K (right). The grey area represents the Rossby scale height (left axis) in Kelvin with an uncertainty marge of 10% due to the size of the polar vortex. The orange curve represents the square of the static stability parameter, N^2 (right axis) in s^{-2}. Both quantities are averaged between 65-89°N.

4.2 2009

In 2009, a SSW took place on 24 January, After 4 days, it already satisfied the conditions of a DSW, so the Centrale Date is on 28 January 2009.

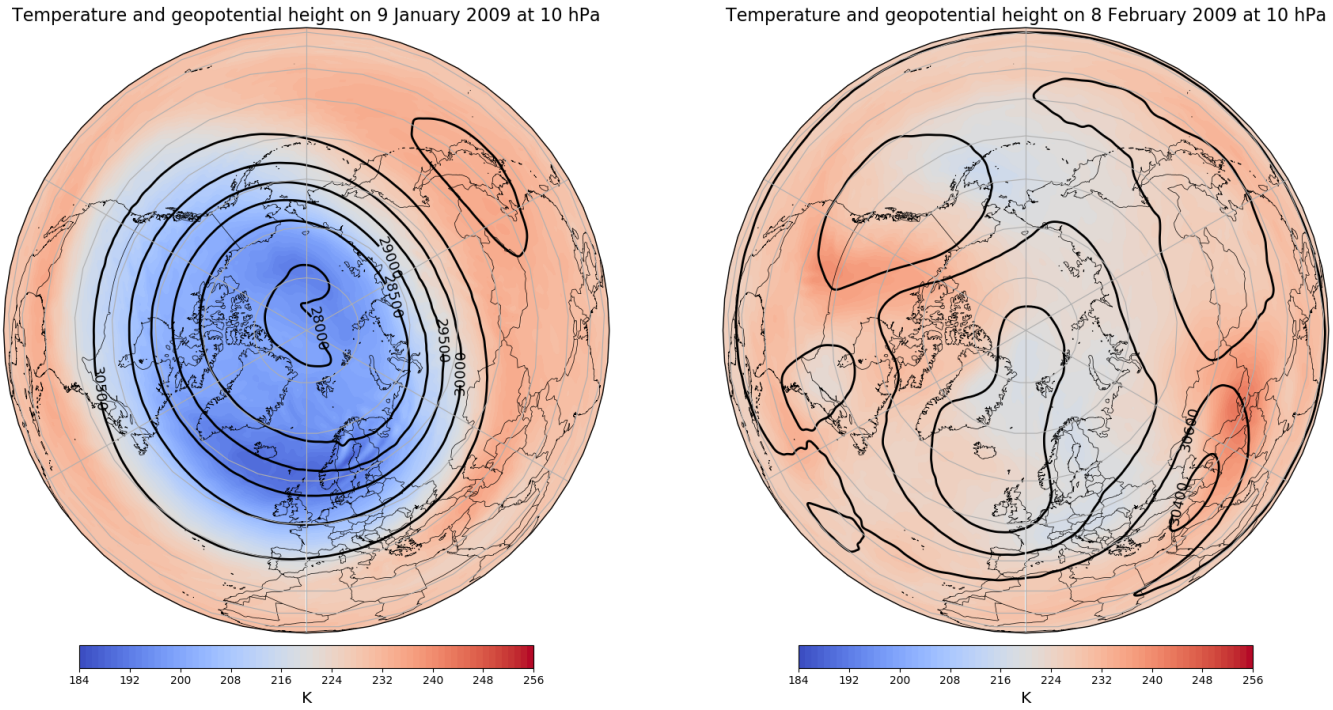

Figure 10: As Figure 4, but now for the SSW of 28 January 2009.

15 days before the SSW, on 9 January 2009 (Figure 10, left panel), the polar vortex is large with its centre above the Arctic Ocean, close to the North Pole. It is filled with cold air over a large area and the horizontal temperature gradients are strong. It is very axisymmetric and thus very strong.
On 8 February 2009, 15 days after the SSW (Figure 10, right panel), the map is pretty chaotic: it looks like that there is one big vortex located above the Atlantic ocean with some pieces around it: it is hard to say if the pieces around the big vortex are also vortices or not. The biggest one is centred above the Atlantic Ocean. The horizontal temperature gradients are significantly reduced.

2. Tropospheric reaction

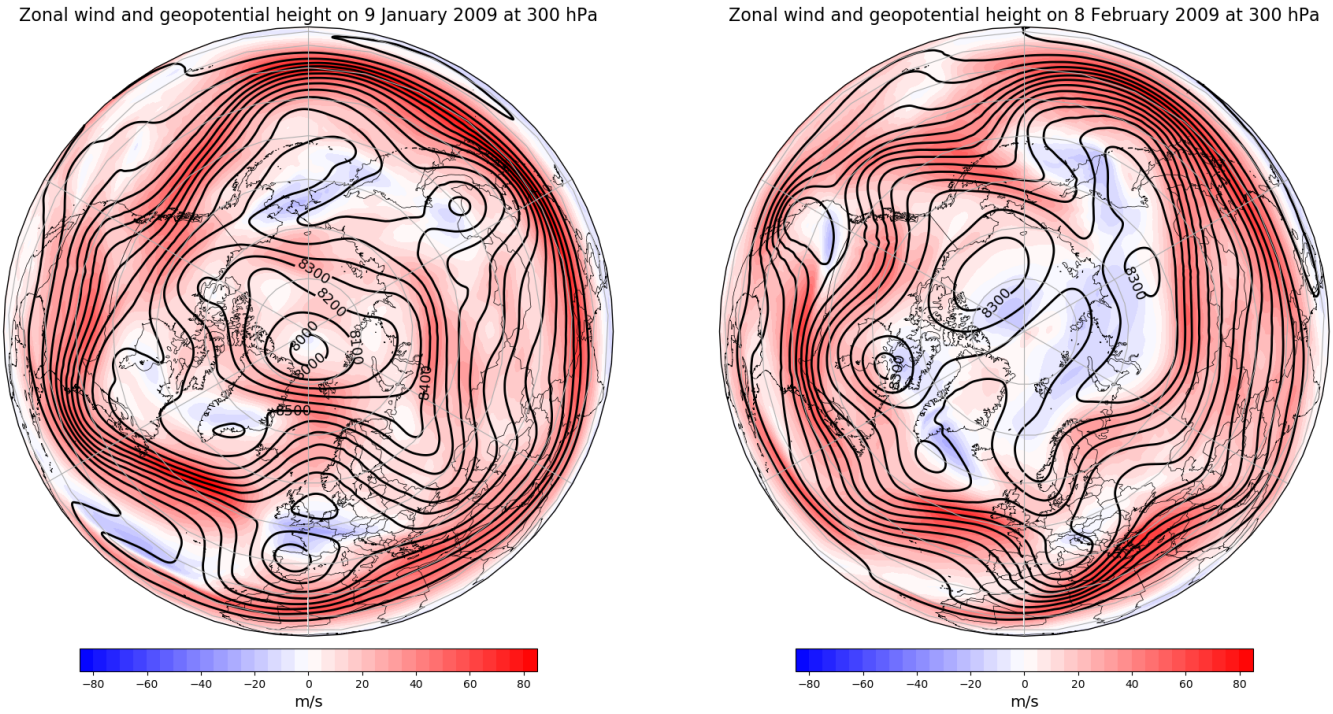

Figure 11: As Figure 5, but now for the SSW of 24 January 2009.

Figure 11 shows the zonal mean zonal wind and geopotential height at 300 hPa. On 9 January 2009 (left panel), 15 days before the SSW, a relatively northern jet (above Scandinavia) with some meanders can be obtained and easterlies above South-Europe. Above the Western-European continent, the geopotential heights are relatively high while over a large area around the North Pole, the geopotential heights are low: this is a relatively northern westcirculation.
30 days later, on 8 February 2009, the jet has significantly displaced equatorwards and flows now above Western-Europe. Easterlies are found in a big area at northern latitudes. The geopotential heights are low there, while they are high above Alaska.

3. The SSW-DSW event

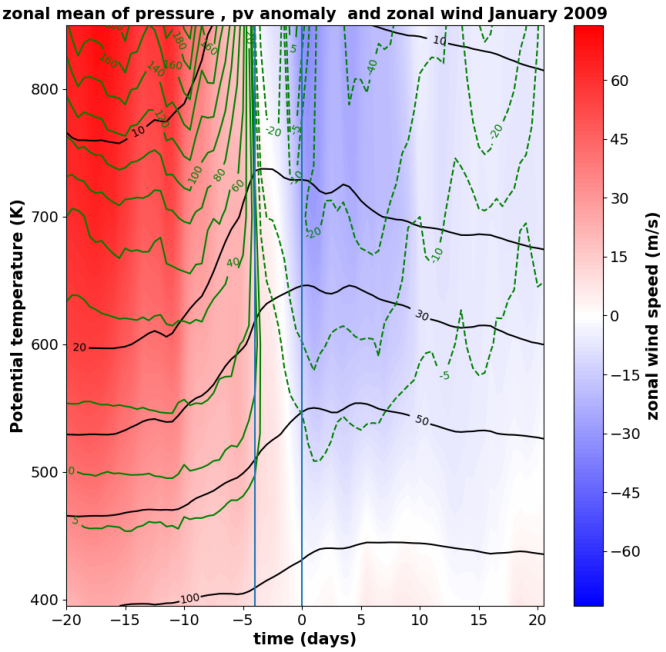

Figure 12: As Figure 6, but now for the SSW of 24 January 2009. The first vertical blue line corresponds to the SSW date (24 January 2009), the second blue line to the DSW date (28 January 2009).

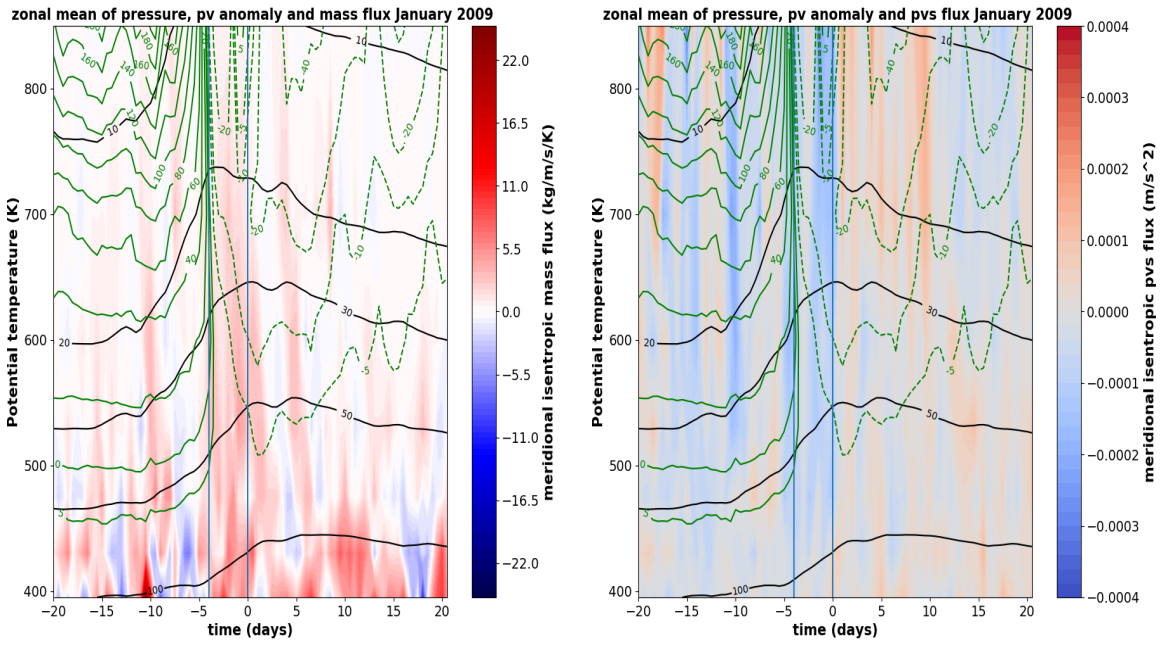

(a) Isentropic mass flux

(b) PVS flux

Figure 13: As Figure 12, but now for the SSW of 24 January 2009.

In Figure 12, the zonal mean zonal wind speed, PV anomalies and isobars are shown for this event. Considering the zonal wind, a clear barrier between positive and negative zonal winds can be seen. Before the first day of

the SSW, the zonal wind is strongly positive and after the SSW it becomes strongly negative. This clearly coincides with the sign of the PV-anomalies; before the SSW, there is a positive PV-anomaly and during the SSW, it becomes negative. The anomalies reach a depth of approximately 450K.
The isobars clearly raise before the SSW and fall some days after the SSW date. From this, it can be derived that the pressure increases significantly during the SSW. The pressure increase ceases in the upper stratosphere while in the lower stratosphere the pressure increases till some days after the CD.

In Figure 13, the mass and PVS fluxes are shown. In the days before the SSW, the mass flux fluctuates in the lower stratosphere while it is close to zero (slightly negative) in the upper stratosphere. Between the first day of the SSSW and the CD, the mass flux becomes positive over the whole vertical layer and it stays mainly positive after the Central Date. The strongest fluxes are seen in the lower stratosphere.
The PVS flux in Figure 13b shows a different behavior. It has also a fluctuating pattern but before the SSW it is mainly negative. After the Central Date of the DSW, the PVS flux turns to mainly positive values, more significantly at larger heights.

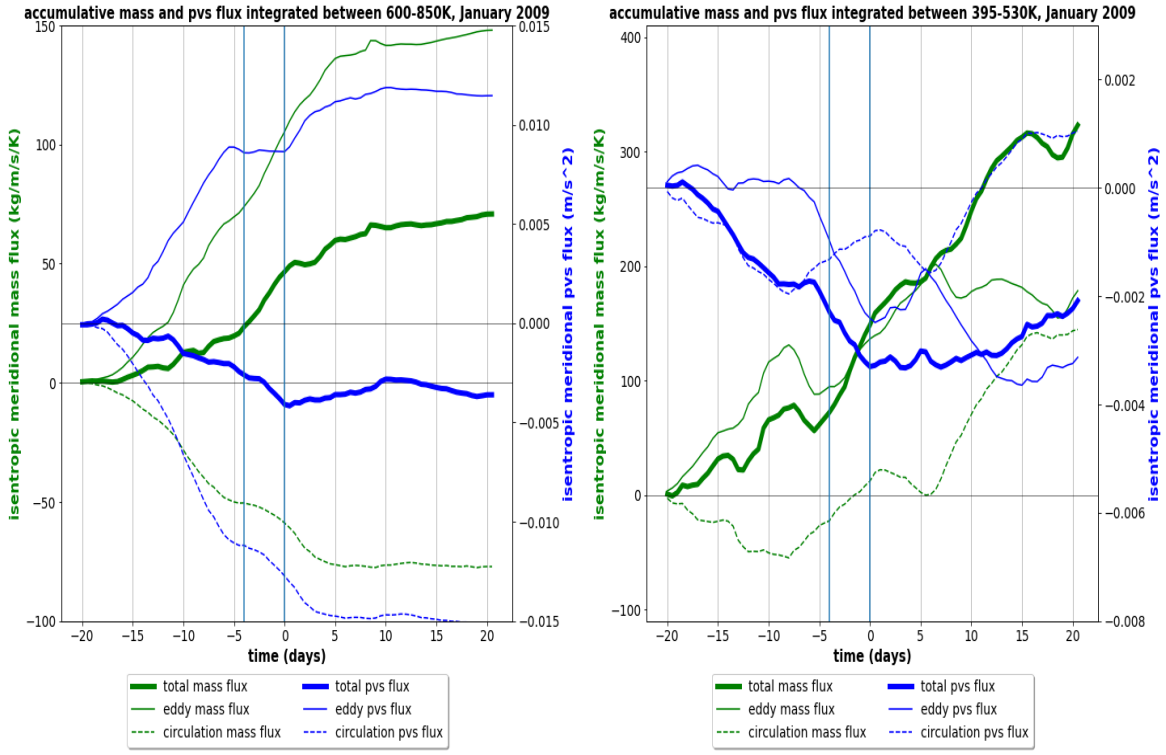

(a) 600-850K

(b) 395-530K

Figure 14: As Figure 8, but now for the SSW of 24 January 2009

In Figure 14a, the accumulated fluxes integrated between 600-850K are plotted. The mass flux starts to increase steadily during the first days, with a stronger increase after the SSW date. After the CD, the growth slowly ceases but in the end, the net flux is constant. The eddy mass flux is positive while the mean circulation flux is negative, but the eddy flux is clearly more dominant. The accumulative PVS flux decreases till the CD. The mean circulation flux is thus generally more dominant than the eddy PVS flux, after the CD it is more in equilibrium. In the end, the net PVS flux is negative.
Figure 14b shows the same but now integrated over a layer between 395-530K. Shortly before the CD, the accumulative mass flux increases strongly while the total PVS flux decreases. Both the eddy and mean circulation mass fluxes are positive during this phase and later, contributing a lot to the total mass flux. The eddy mass flux is more dominant the whole period. For the PVS flux, both the eddy and mean circulation fluxes are negative, where the contribution due to eddies is stronger. The mean circulation flux increases and becomes positive, making the total PVS flux to increase eventually.

4. Rossby height and static stability

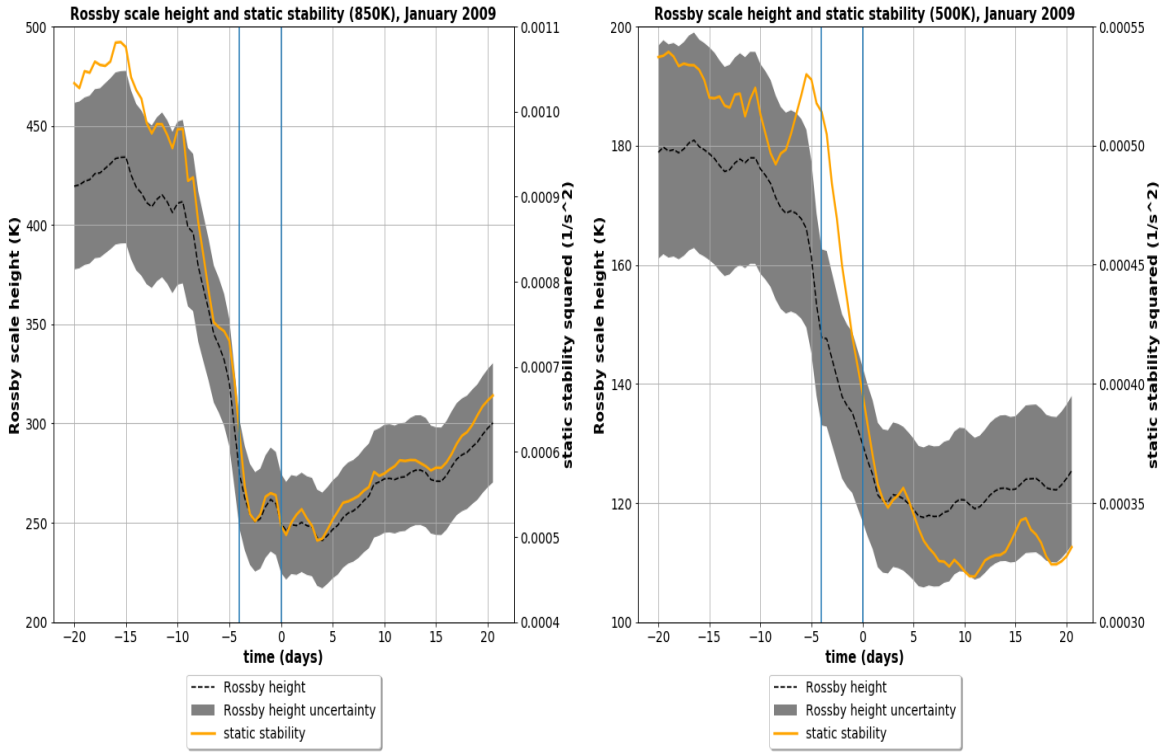

(a) 850K (b) 500K

Figure 15: As Figure 9, but now for the SSW of 24 January 2009.

At 850K, both the Rossby height and static stability are high initially; they start to decrease rapidly 10 days before the first day of the SSW. They both reach their minimum values shortly after the CD and increases slightly afterwards.
At 500K, we see roughly the same pattern: the big drop in Rossby height and stability sets in a few days later as well as the time the minima are reached: around day +10.

4.3 2013

In 2013, a SSW of the split type took place on January the 6th which was followed by a DSW on January the 18th.

1. The polar vortex state

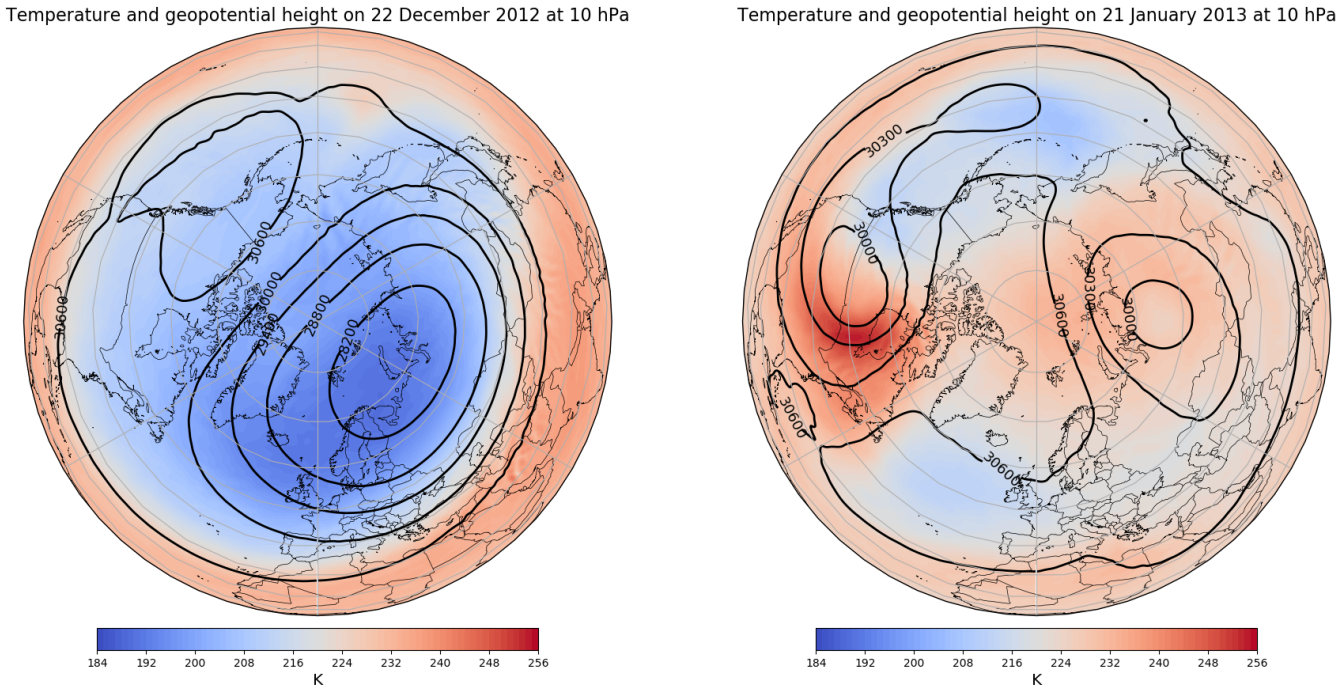

Figure 16: As Figure 4, but now for the SSW of 6 January 2013.

In the left panel of Figure 16, the polar vortex 15 days before the SSW is shown. The vortex is settled above the Barents sea. It spans from the East of Canada to the Asian continent and is quite axisymmetric. A large cold pool is enclosed in it.
15 days after the SSW (Figure 16, right panel), the vortex has split up into two parts, a warm one with the core above North-America and a colder one with the core above Siberia. The horizontal temperature gradients are reduced.

2. Tropospheric reaction

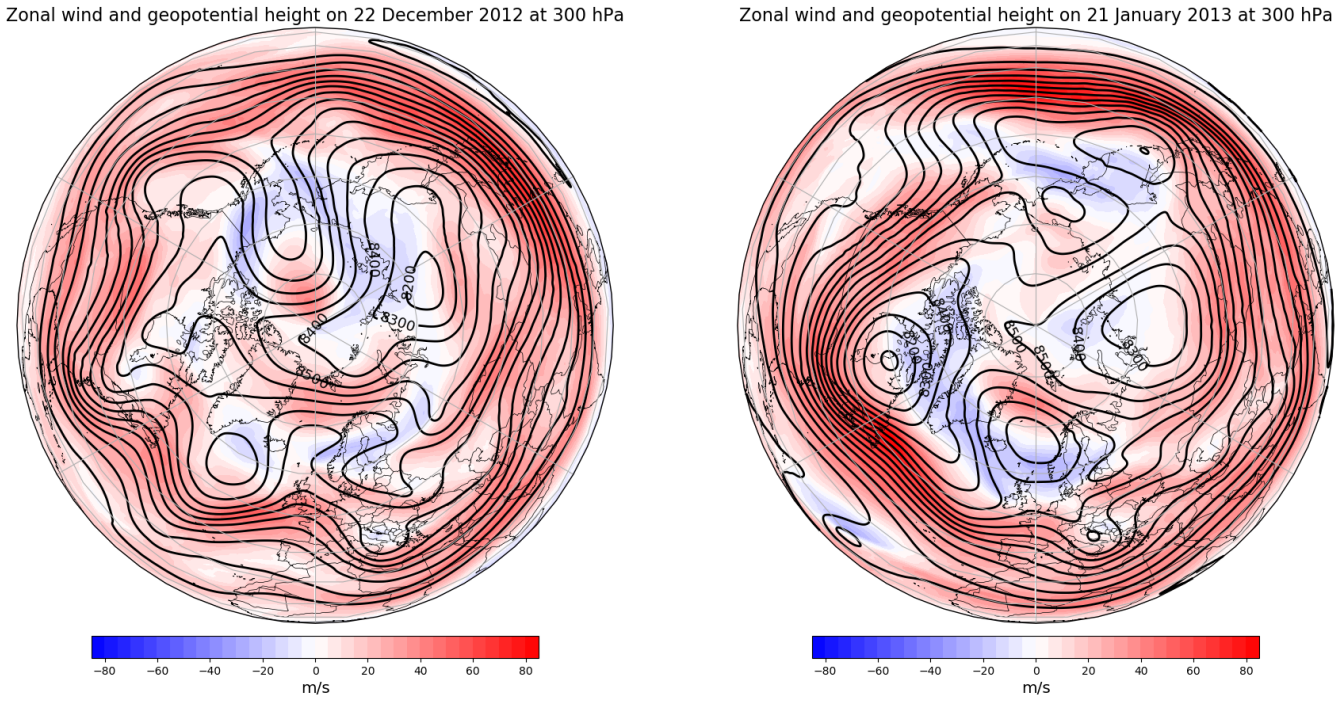

Figure 17: As Figure 5, but now for the SSW of 6 January 2013.

Figure 17 shows the zonal mean zonal wind and geopotential height at 300 hPa. On 22 December 2012, 15 days before the SSW, the jet stream is strong and flows over Western-Europe, but there are some meanders. Above Scandinavia and Iceland, the zonal wind is negative. The geopotential heights are relatively low above the Atlantic Ocean and Eastern-Siberia and high at northern latitudes, between 70 and 80 $°N$.
15 days after the SSW, on 21 January 2013, the jet has shifted equatorwards. Above Northern and Western Europe, the winds are easterly. Large geopotential heights are located above Scandinavia and Greenland while low geopotential heights are located above Siberia and Northern-America. A block above the northern Atlantic Ocean is the result.

3. The SSW-DSW event

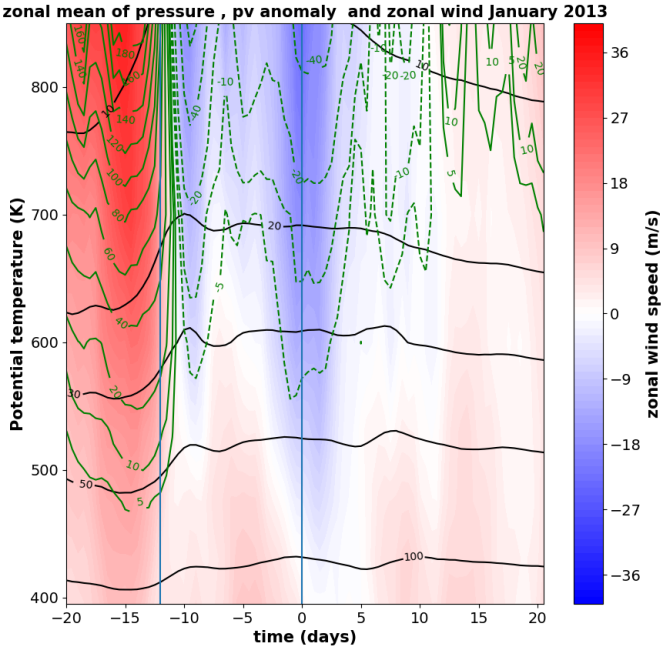

Figure 18: As Figure 4, but now for the SSW of 6 January 2013. The first vertical blue line corresponds to the SSW date (6 January 2013), the second blue line to the DSW date (18 January 2013).

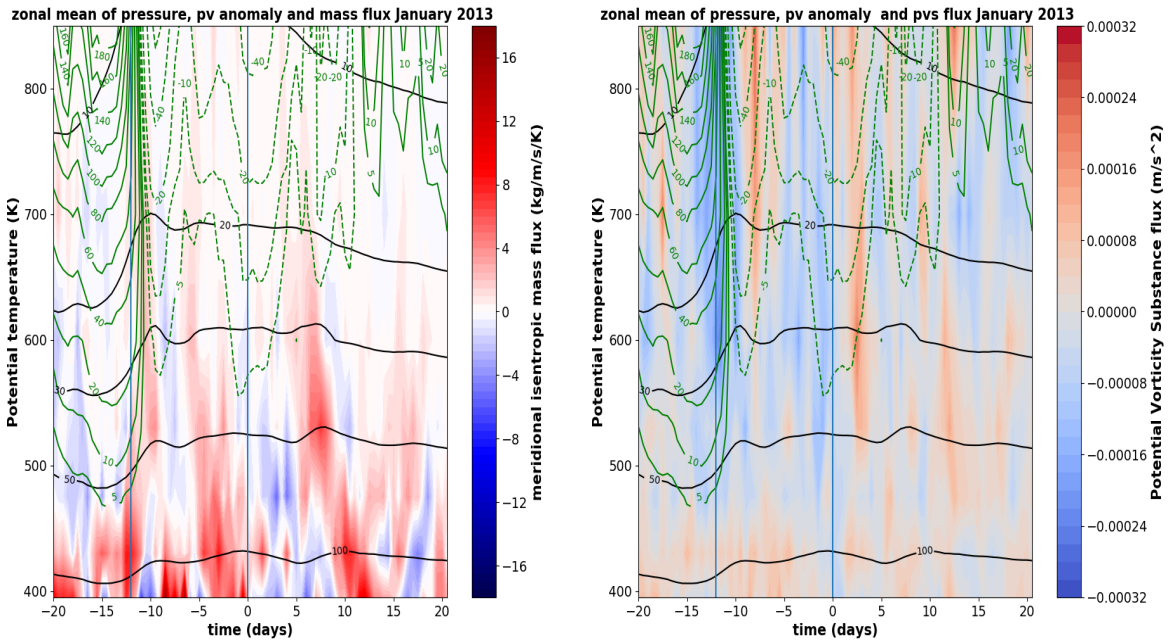

(a) Isentropic mass flux

(b) PVS flux

Figure 19: As Figure 7, but now for the SSW of 6 January 2013.

The zonal mean zonal wind speed, PV anomalies and isobars of January 2013 are plotted in Figure 18. Starting with the zonal wind, the same pattern as the previous cases can be observed: before the SSW date,

the zonal mean zonal wind is positive and during the SSW the zonal mean zonal wind turns to negative values till day 9 after the CD, with exception of a small band of positive winds around day -8. The wind speed has clearly a minimum at the CD.
Also the isobars show similar behavior. Before the SSW they raise, more significantly in the mid stratosphere, and during the the SSW they start to lower from above. Around day -9, there is a small dip in the pressure.
The PV-anomalies are strongly positive before the SSW date, and negative during the SSW. After day +14, the PV-anomaly gets positive again from above. The minimum PV-anomaly is reached around the CD at a level of 500K (60 hPa). There is a striking zone of slightly positive zonal winds while the PV-anomaly is still negative between day +10 and +14.

Considering the fluxes of the isentropic mass in Figure 19a, a fluctuating pattern which tends towards positive values can be seen. This signal is also stronger in the lower stratosphere (< 600K) than in the upper stratosphere. It seems that a there where the PV-anomalies are positive, the mass flux is negative and vice versa.
The PVS-flux is shown in Figure 19b. Before and on the first days of the SSW, the PV-flux is negative. Between day -12 and +15, it seems that the flux fluctuates strongly between positive and negative values. After day 15, the PVS flux becomes mainly negative.

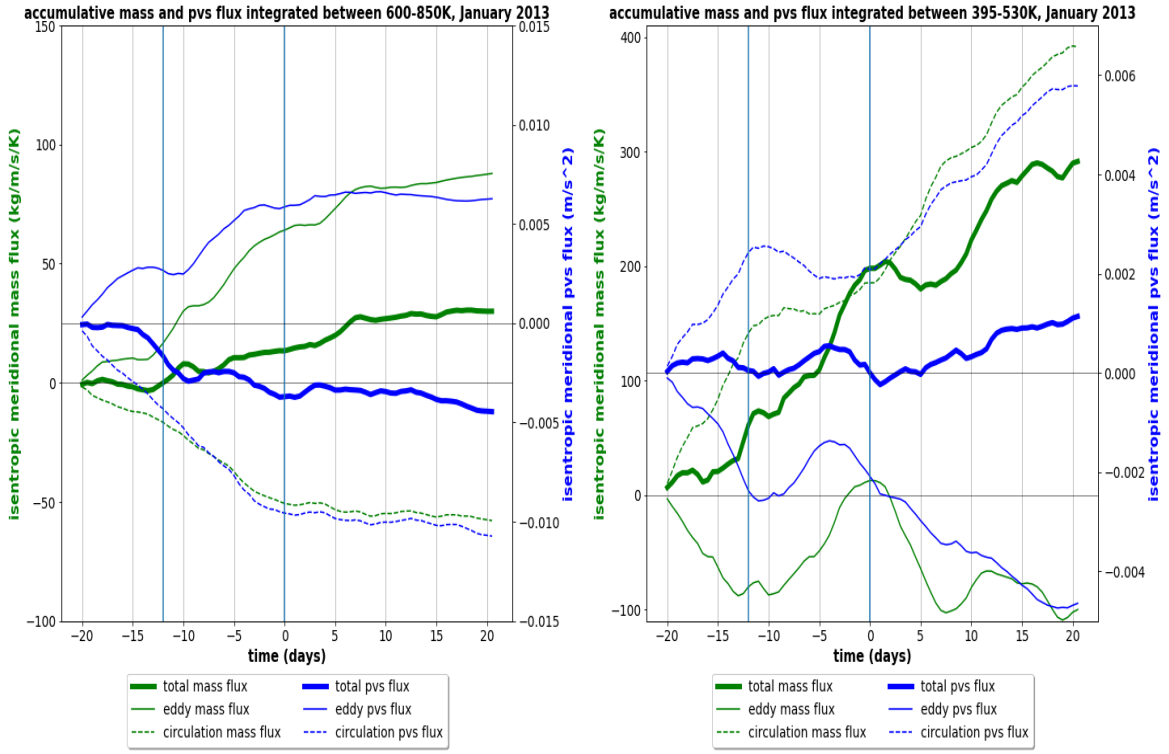

(a) 600-850K

(b) 395-530K

Figure 20: As Figure 8, but now for the SSW of 6 January 2013.

In Figure 20a, the integrated accumulative isentropic mass and PVS flux integrated between 600-850K are shown. Some days before the SSW, the mass flux increases while the PVS flux decreases. A few days later, the mass and PVS fluxes have a little dip respectively peak. Eventually, the net mass flux is positive and the net PVS flux is negative.
Looking at the eddy and mean circulation components of the fluxes, the same pattern as in the previous cases is visible. Just before and later, both mass and PVS eddy fluxes increases while the flux due to the mean circulation decreases. After the CD, the changes in both fluxes become small.
Figure 20b shows the same as Figure 18a but now integrated over a layer between 395-530K. About five days before the CD, the accumulative mass flux increases significantly. Meanwhile, the total PVS flux decreases. The mean circulation mass flux is positive and increases during this whole period while the eddy flux is negative and decreases, this holds for both the mass and PVS flux. The mean circulation fluxes are more dominant than the eddy fluxes since both the net total mass and PVS flux are positive in the end.

4. Rossby height and static stability

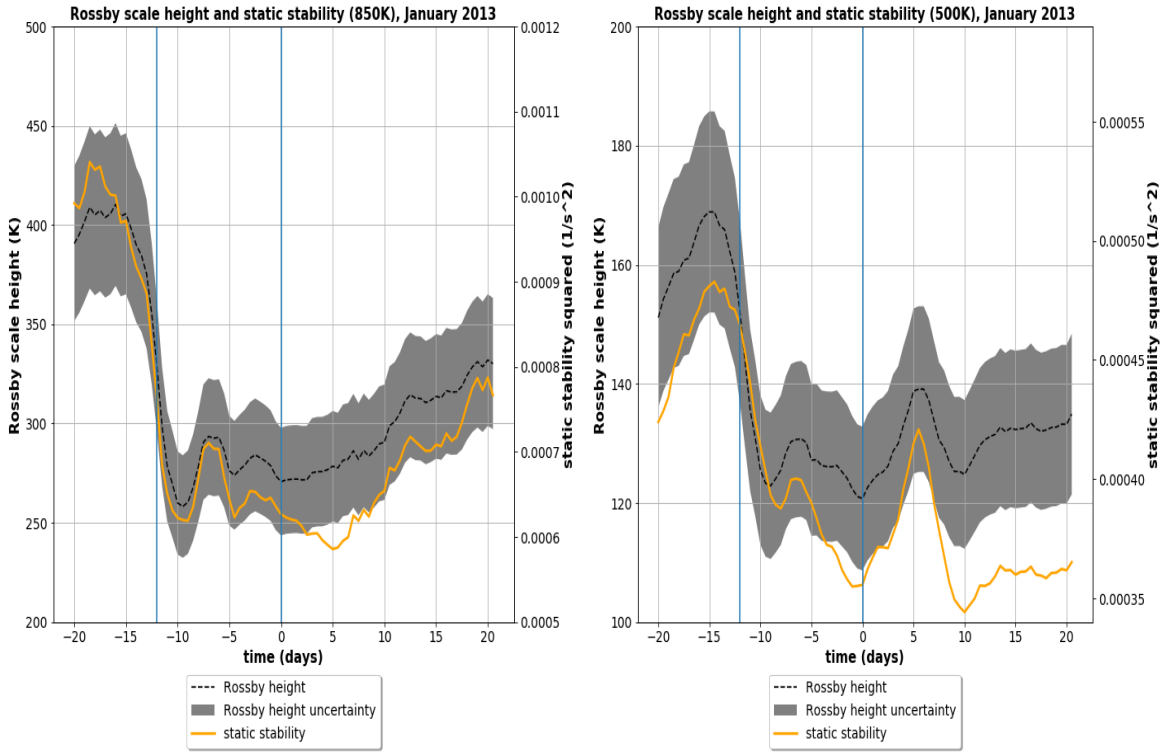

(a) 850K (b) 500K

Figure 21: As Figure 9, but now for the SSW of 6 January 2013.

In Figure 21a, the Rossby scale height and static stability at the 850K level are plotted. Both quantities are initially high but start to drop rapidly some days before the SSW. The Rossby height reaches its minimum just after the SSW, the static stability 5 days after the CD. They both increase gradually after day 5.
At 500K (Figure 21b), the Rossby height and stability increases initially and reach a maximum before it starts to decrease quickly. Both the Rossby height and stability have a dip just before the CD and stay relatively low with exception of a peak 5 days after the CD. The stability reaches its absolute minimum after that peak.

4.4 2018

On 12 February 2018, the criteria of an SSW were satisfied. As mentioned earlier, the SSW of February 2018 did not satisfy the criteria of a DSW. Nevertheless, it had a great tropospheric impact as will be shown later. The CD is chosen in such a way that the first day of the SSW occured 10 days before the CD; day -10 corresponds to the first day of the SSW.

1. The polar vortex state

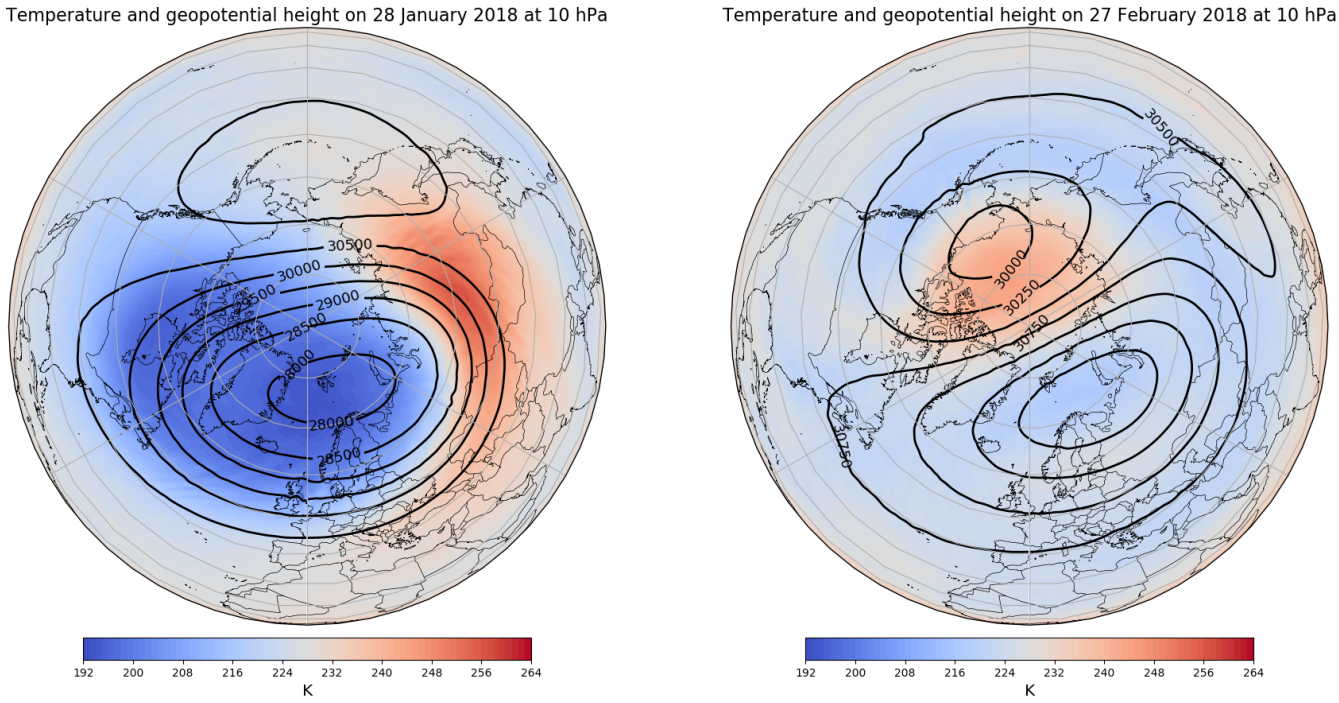

Figure 22: As Figure 4, but now for the SSW of 12 February 2018.

On January the 28th, the polar vortex is centred roughly around Svalbard. It stretches from halfway Northern America to Siberia. It has a large cold area and there is some heat advection on the right edge of the vortex. It is pretty axisymmetric and thus at this stage, the polar vortex is relatively strong.
On February the 27th, the vortex has split into two parts: a small one with a warm core above the Arctic Sea above Alaska and a large one with a cold core above the Barents sea. Also noticeable is the reduced horizontal temperature gradient: especially the initially cold air is much less cold 15 days days after the SSW.

2. Tropospheric reaction

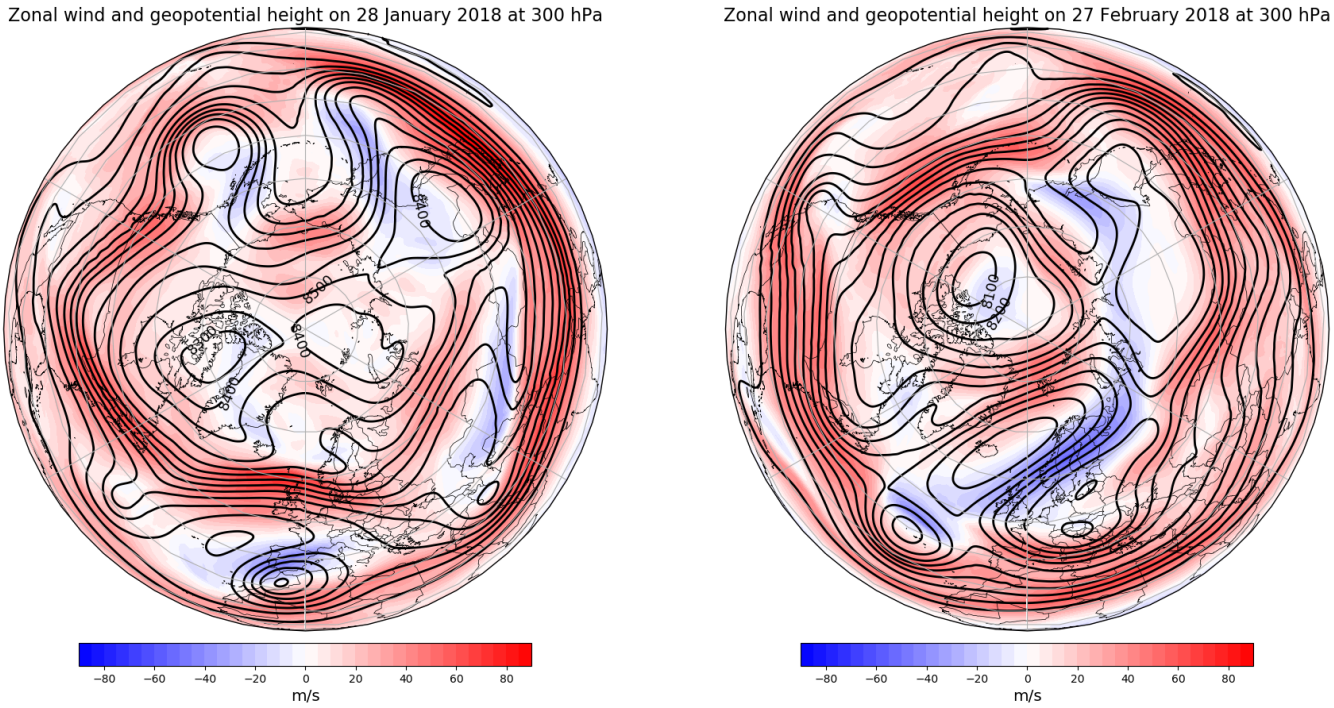

Figure 23: As Figure 5, but now for the SSW of 12 February 2018.

Figure 23 shows the zonal mean zonal wind and geopotential height at 300 hPa. On 28 January 2018 (left panel), 15 days before the SSW, the jet is very strong and located above Western Europe has no meanders. Above Southern-Europe, the zonal winds are easterly. High geopotential heights are located above Mid- and Southern-Europe and low geopotential heights above Greenland and around the North Pole. This is a typical westcirculation.
On 27 February 2018 (right panel), 15 days after the SSW, the jet stream has displaced equatorwards, above Southern-Europe. Easterlies flow over large parts of Europe. The geopotential heights are low above the Arctic Ocean and high around a large area around the North Pole. This is a very strong blocking.

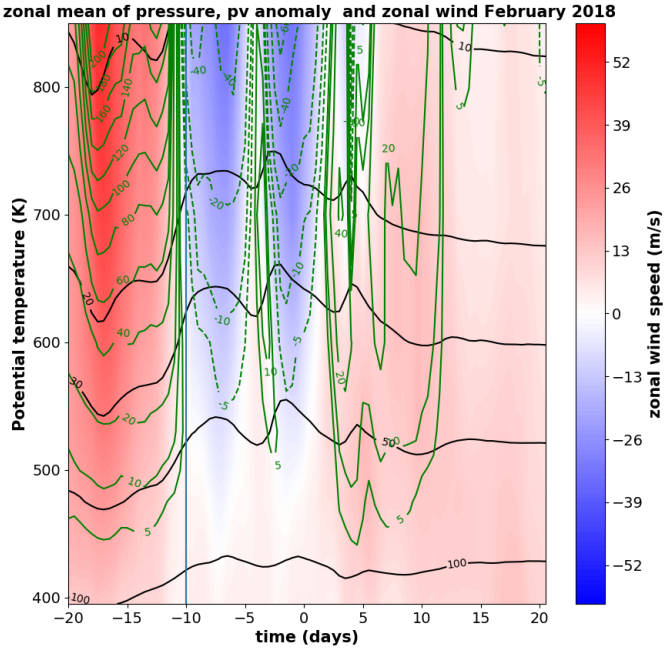

Figure 24: As Figure 6, but now for the SSW of 12 February 2018. The vertical blue line corresponds to the SSW date (12 February 2018).

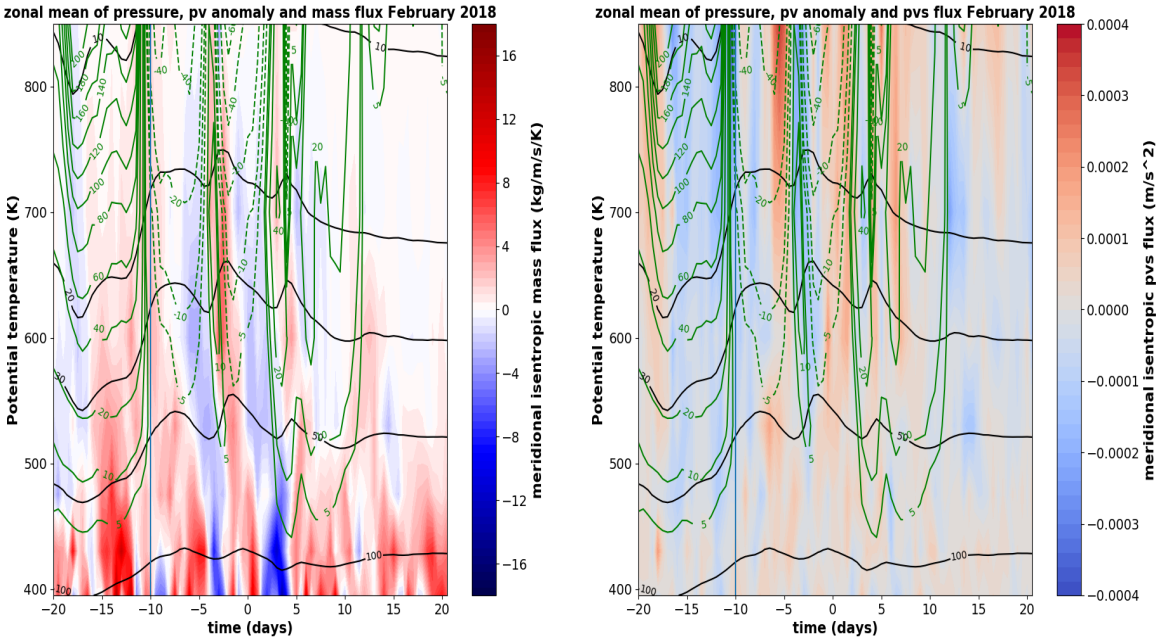

(a) Isentropic mass flux

(b) PVS flux

Figure 25: As Figure 7, but now for the SSW of 12 February 2018.

The zonal mean zonal wind (Figure 24) is strongly positive before the SSW and becomes instantaneously negative during the SSW. There is a 'double dip' in this negative wind peak before it gets positive again later,

around the CD. The same holds for the PV anomaly evolution. The anomalies become negative at the SSW date and reach a lowest level of 530K (50 hPa) and is positive elsewhere.
The pressure decreases in the first few days but later the pressure starts to increase. The pressure keeps on increasing during the SSW. The isobars show some fluctuations in this period.

The mass flux, shown in Figure 25a, is mainly positive over the whole vertical layer.
The PVS flux, shown in Figure 25b, is negative in the days before the SSW (except from the first 2 days) and after the SSW it seems that it, unlike the previous cases, becomes mainly positive.

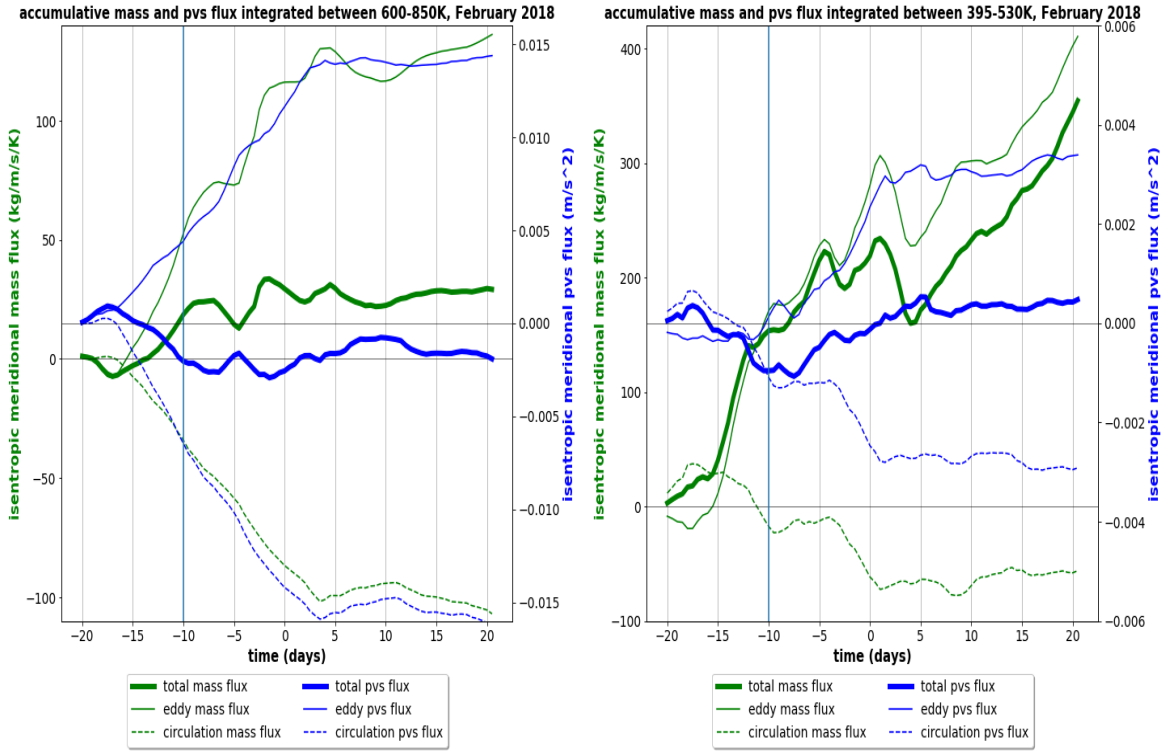

(a) 600-850K

(b) 395-530K

Figure 26: As Figure 8, but now for the SSW of 12 February 2018.

Figure 26a shows the accumulated fluxes integrated between 600-850K. The accumulated total mass flux increases in the days before the SSW takes place and shows then a further increase alternated with some short periods of decay, corresponding to the negative mass fluxes seen in Figure 25a. The eddy mass flux dominates the mean circulation flux, leading to a positive net mass flux in the end. The accumulative total PVS flux shows almost exactly the opposite behavior as the mass flux. The only difference is that the net PVS flux is slightly negative in the end, due to a stronger zonal mean circulation.
Figure 26b shows the same but then integrated between 395-530K. Some days before the CD (on 21 February 2018, remember that there was no DSW in 2018), the total accumulative mass flux increases rapidly. Meanwhile, the total accumulative PVS flux decreases. In the end, both the net mass and PVS flux are positive. The fluxes due to mean circulation are dominant most of the time.

4. Rossby height and static stability

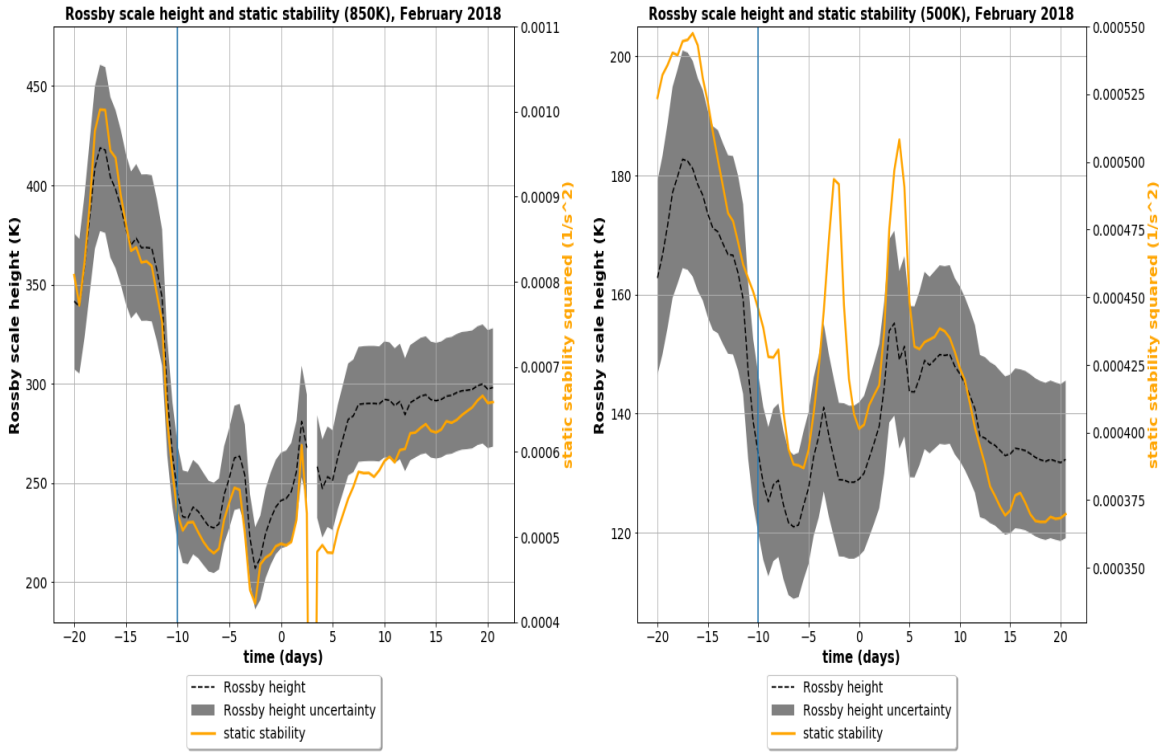

(a) 850K (b) 500K

Figure 27: As Figure 9, but now for the SSW of 12 February 2018.

Figure 27a shows the static stability and Rossby height at 850K. Both reach a maximum 6 days before the SSW, then decrease till the SSW date, have a second peak some days after the SSW and drop then rapidly afterwards. There are multiple minima during this period.[14]
At 500K (Figure 27b), both the Rossby height and stability parameter are initially relatively high with a maximum some days after the SSW. Both quantities decrease suddenly after that maximum and quickly reach their minimum. Peaks and dips alternate then with but with an increasing tendency.

[14]On day +13, the static stability at 850K has a very low value which is not displayed in the figure. Since this value is an extreme outlier compared to the others values and other cases, this value is omitted.

4.5 2019

The most recent SSW occurred on 1 January 2019, followed by a DSW on 16 January 2019. It led to a split of the polar vortex.

1. The polar vortex state

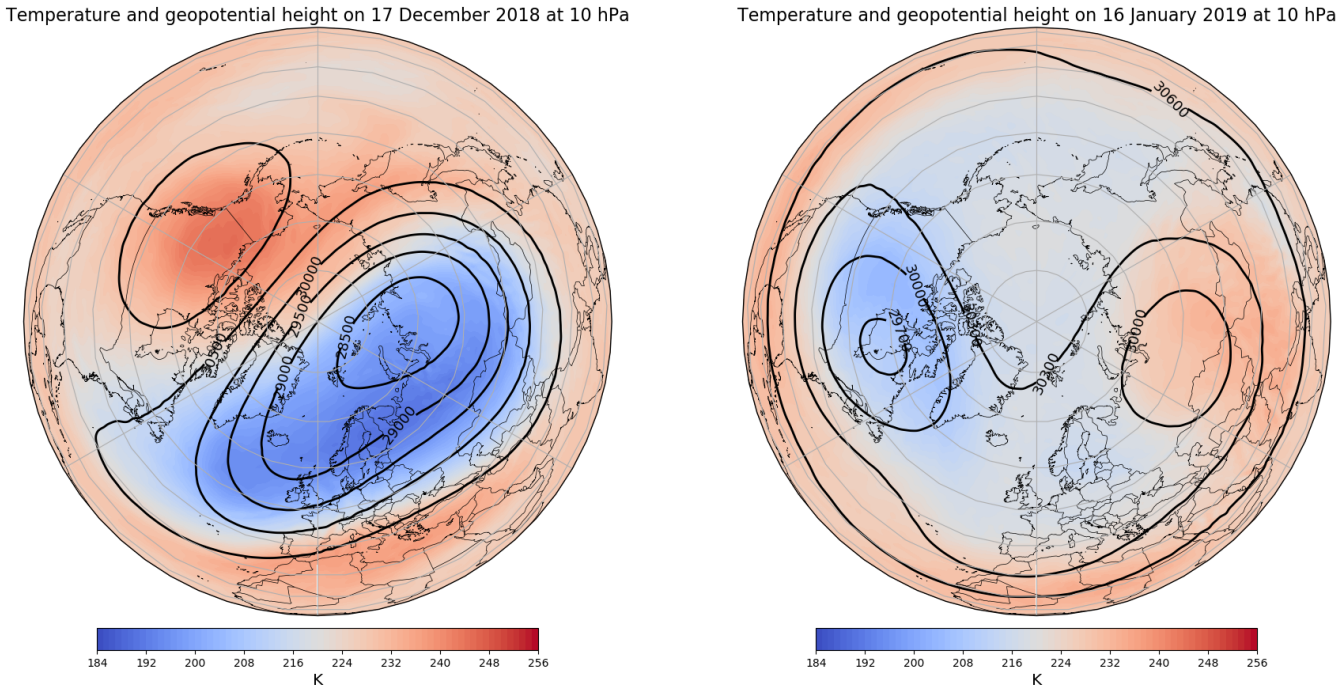

Figure 28: As Figure 4, but now for the SSW of 1 January 2019.

On 17 December 2018, 15 days before the SSW (Figure 28, left panel), the polar vortex is a bit elongated with its core above northern Siberia. The horizontal temperature gradients are strong.
On 16 January 2019, 15 days after the SSW (Figure 28, right panel), the vortex has split up into two daughter vortices. One vortex with cold air is located above Canada and the other vortex with warmer air above Siberia. The horizontal temperature gradients are reduced.

2. Tropospheric reaction

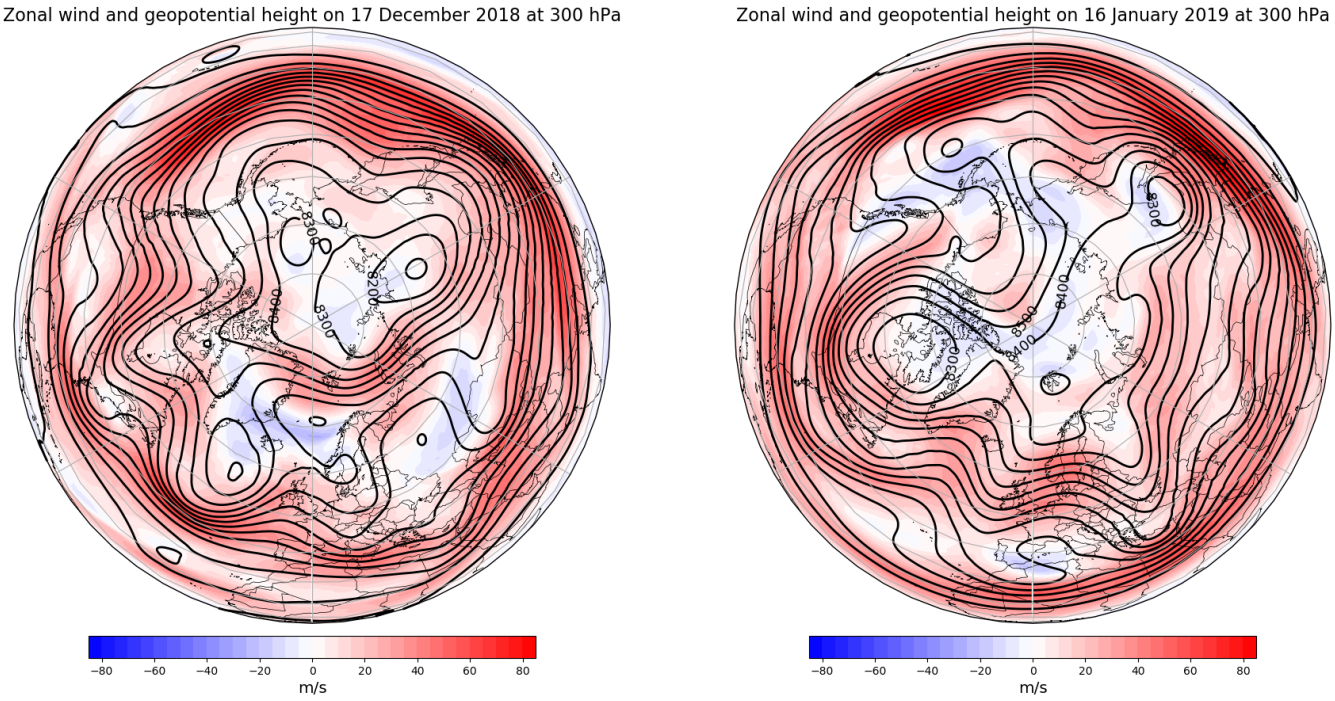

Figure 29: As Figure 5, but now for the SSW of 1 January 2019.

Figure 29 shows the zonal mean zonal wind and geopotential height at 300 hPa. On 17 December 2018 (left panel), 15 days before the SSW, the jet is relatively strong and has some meanders. Above the Northern Atlantic Ocean and Greenland, the winds at 300 hPa are easterly. Around the North Pole, the geopotential heights are low as well as above Russia and Scandinavia.
On 16 January 2019 (right panel), 15 days after the SSW (and on the CD), the jet is still strong and has shifted northward, with some relatively strong meanders. Above Southern-Europe, the winds are easterly. In a large area around the North Pole, the geopotential height is low. High geopotential heights are located above Eastern-Siberia.

3. The SSW-DSW event

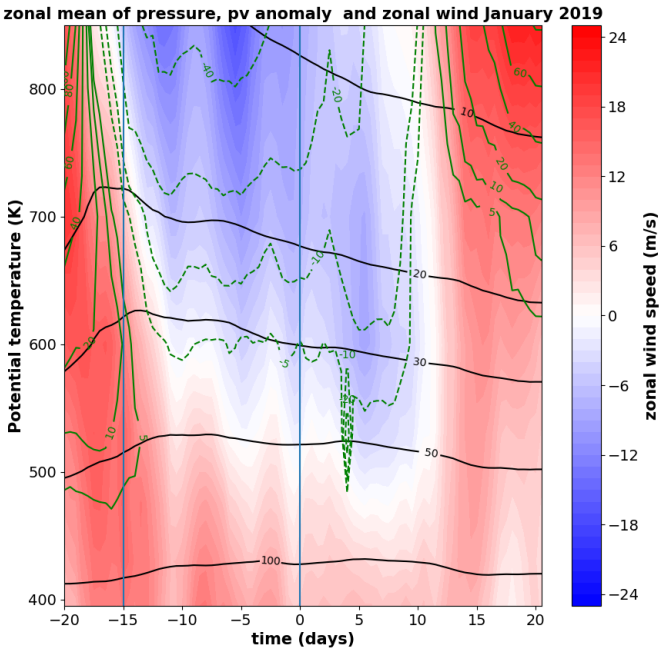

Figure 30: As Figure 6, but now for the SSW of 1 January 2019. The first vertical blue line corresponds to the SSW date (1 January 2019) and the second line to the DSW (16 January 2019).

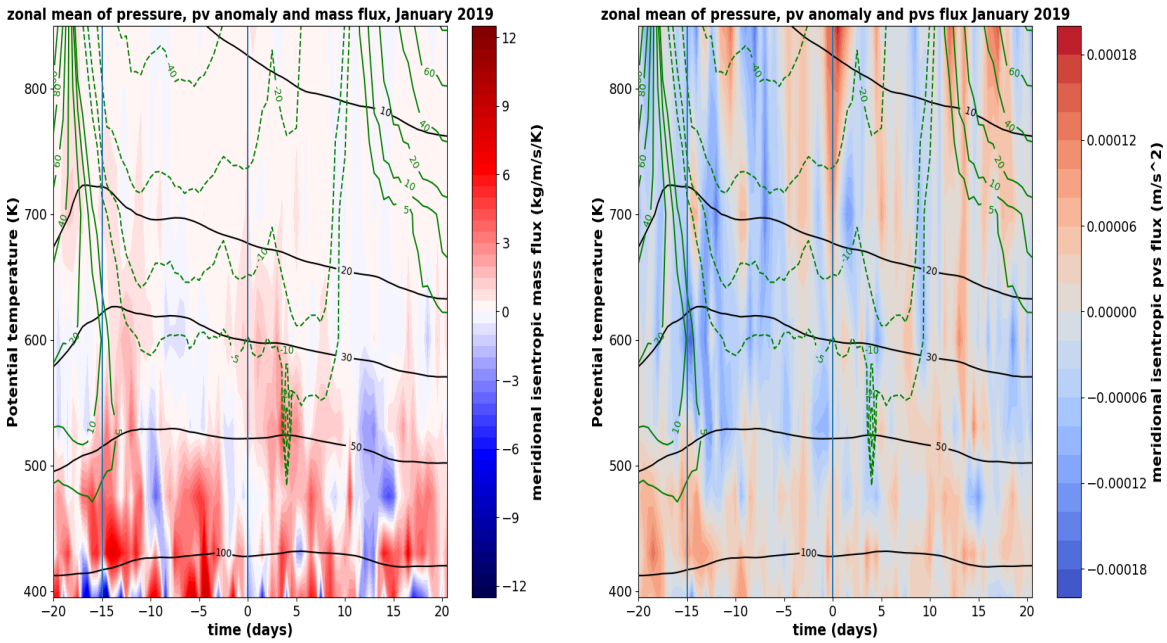

(a) Isentropic mass flux

(b) PVS flux

Figure 31: As Figure 7, but now for the SSW of 1 January 2019.

The zonal mean zonal wind, PV-anomaly and pressure is shown in Figure 30. The zonal mean zonal wind is initally positive. After the SSW, it becomes negative till day +10 and restores abruptly to positive values.

The PV-anomaly fits the negative zonal wind field very well. Positive PV-anomalies correspond to positive zonal winds and negative PV-anomalies to negative zonal winds. The negative PV-anomaly has a maximum depth of about 50 hPa, some days after the CD.
Before the SSW, the isobars raise quickly and after the SSW the isobars gradually lower.

In Figure 31, the isentropic mass and PVS fluxes are plotted. The mass flux is mainly positive, especially around both the SSW and DSW date. The strongest fluxes are like the other cases in the lower stratosphere. The PVS flux fluctuates, but is mainly negative above 500K (50 hPa). Below 500K, it seems that there is a mainly positive PVS flux. Also around and after the CD, there are some moments of intense PVS fluxes in the upper stratosphere.

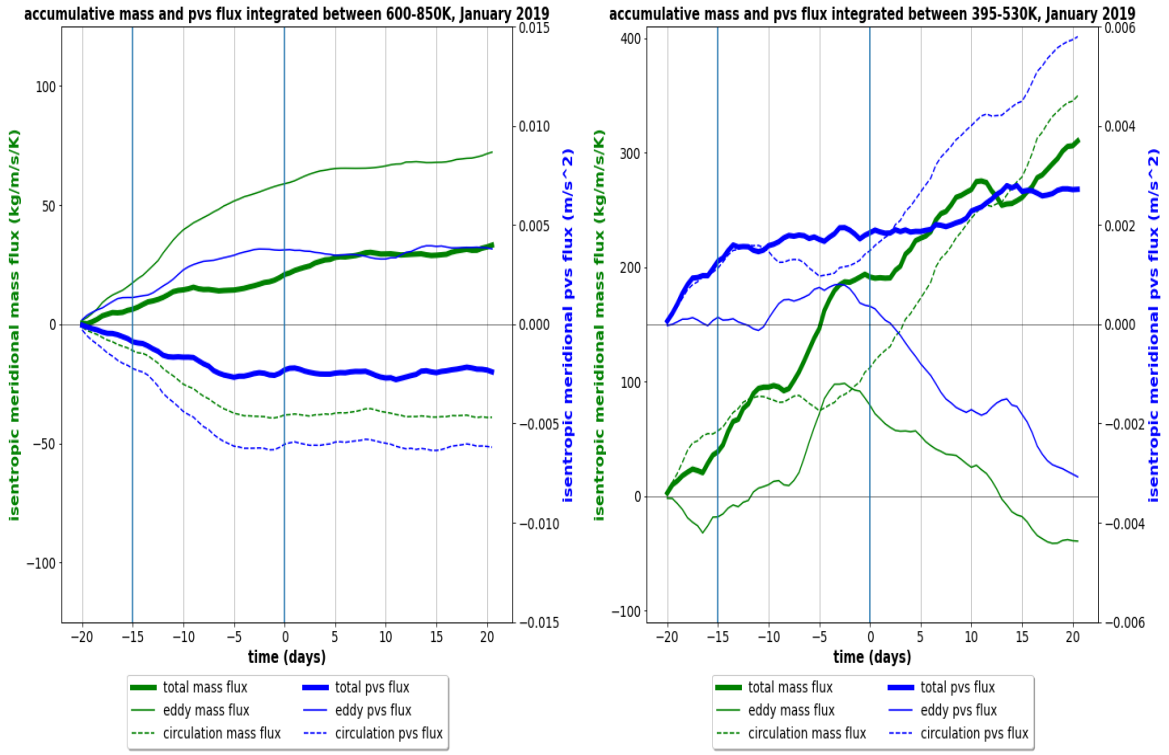

(a) 600-850K

(b) 395-530K

Figure 32: As Figure 8, but now for the SSW of 1 January 2019.

Figure 32a shows the accumulative mass and PVS flux and the eddy and mean circulation parts integrated over a layer between 600-850K. The accumulative mass flux shows an increasing trend, which is the strongest in the days before the SSW and ceases after the DSW. Both the eddy and mean circulation flux grow significantly till some days before the CD, after the CD the changes are small. The eddy fluxes clearly dominate over the mean circulation flux since the net accumulative mass flux is positive during the whole period. The reverse happens to the PVS flux and its eddy and mean circulation components. The only difference is that the mean circulation PVS flux is stronger than the eddy PVS flux since the net accumulative PVS flux is negative.
Figure 32b shows the same but now integrated over a layer between 395-530K. In the period between the SSW date and the CD, the total mass flux increases significantly, while the changes in the total PVS flux are small. Eventually, both the net mass and PVS fluxes become positive. This is due to the increase of the mean circulation mass and PVS flux, which starts some days before the CD. Both eddy fluxes decrease and become negative.

4. Rossby height and static stability

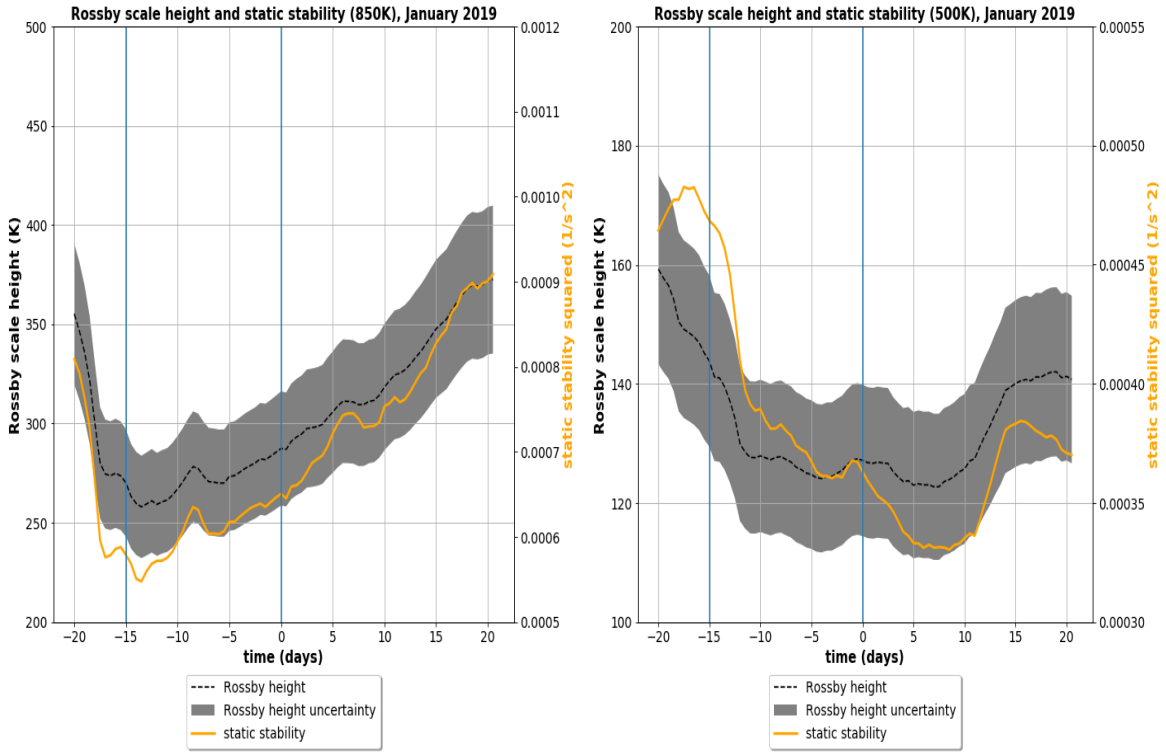

(a) 850K (b) 500K

Figure 33: As Figure 9, but now for the SSW of 1 January 2019.

In Figure 33a, the Rossby height and static stability at 850K are shown. Before the SSW, the Rossby height and static stability are high but are already decaying and reach their minimum shortly after the SSW. They both increase steadily afterwards.
At 500K (Figure 33b), both parameters decrease steadily till approximately 10 days after the CD and are followed by a short but steep increase.

5 Discussion of the case studies

5.1 The results explained

Based on the results of the previous section, the following statements can be made:

1. Positive zonal mean PV anomalies coincide with a positive (westerly) zonal mean zonal wind speed and negative PV anomalies coincide with a negative (easterly) zonal wind speed, as expected.
2. Before an SSW, the PV anomaly in the mid stratosphere is highly positive; after a SSW, it becomes negative for some time.
3. The PV anomalies reach a level of roughly 450K ($\approx$ 75 hPa), so they do not penetrate the troposphere.
4. During an SSW, the pressure increases significantly throughout the stratosphere and upper troposphere; after a SSW the pressure decreases gradually. Pressure changes are more significant at the larger heights
5. During and after a SSW and DSW, an enhanced poleward mass flux is found in the mid and low stratosphere. The accumulative sum of the total mass flux is positive, which means that eddies are more important than the mean circulation for the mass flux in the mid stratosphere.
6. On the other hand, the total PVS flux is negative and decreases generally after a SSW and DSW, indicating an equatorward PVS flux. Since the accumulative sum is negative, this means that the PVS flux due to the mean circulation is more important
7. Both the eddy and mean circulation component of the mass and PVS flux increase, respectively decrease with time during an SSW. After an SSW, the enhanced mass and PVS flux perturb the mid and low stratosphere; after a DSW, both the eddy activity and mean circulation weakens with time, and the perturbations stop.
8. The static stability decreases quickly during a SSW; reduced stratification may lead to more mixing. After the SSW, the static stability gradually increases again and cancels the negative PV-anomaly, restoring the polar vortex.

All of the statements above will be explained one by one in this section. Cases which show some deviant or unexpected results will also be explained.

1. The coincidence of zonal wind and PV anomalies

This follows directly from the PV-inversion principle, which states that positive PV anomalies induces a cyclonic wind field (positive zonal wind speed) and that negative PV anomalies induces an anticylonic wind field (negative zonal wind speed) and is therefore also adjustment to thermal wind balance. Deviations from this principle are so small that they can be considered as negligible.

2. Positive PV anomalies before SSW, negative PV anomalies after SSW

This can (partially) be explained by the appearance of planetary waves. As explained in section 2.1.1, planetary waves propagate upwards and the ones which reach the polar vortex exchange angular momentum with the zonal wind when they break. If the polar vortex is not too strong, these waves are able to propagate through the vortex. However, they also cause mixing of PV when they break. As long as the zonal wind is positive, the waves break and mix PV causing a positive PV anomaly. At the moment that the vortex displaces or splits, the zonal mean zonal wind becomes easterly and the waves can no longer propagate through the vortex. Negative PV anomalies arise as a result of PV-mixing. On the longer term, the polar vortex recovers; the zonal mean zonal wind becomes westerly again and the planetary waves can propagate through the polar vortex, mixing the PV. A SSW can be physically interpreted as an extreme example of PV-mixing.

3. Pressure changes before and after a SSW

The increase of isentropic pressure before an SSW can be explained by the increased poleward flux of mass, caused by an enhanced meridional mass circulation in the stratosphere. This can be seen in the figures of the accumulative fluxes: in all cases, we see that the mass flux towards the pole increases before the SSW takes place. Another explanation is that from the PV-invertibility principle; it followed that a cold and thus heavy air mass is characterized by a positive PV anomaly above it and that a cold air mass loses the properties of a cold air mass when the PV distribution changes (this concept is called 'Kleinschmidts principle' in this report).

After an SSW the polar PV anomaly becomes negative, which implies that the initially cold air masses inside the vortex become warmer. This warmer air mass sinks eventually, explaining the increase in pressure observed after the SSW. The mass pumped inside the polar vortex can not leave the vortex by horizontal mass transport since the mass flux is still polewards. The only way it can go is downwards, which also explains the pressure increase at lower levels in the stratosphere and upper troposphere which takes place a few days later. The fact that the pressure changes in the mid stratosphere are stronger than in the lower stratosphere and upper troposphere can be explained then simply by the fact that the largest PV anomalies were also found in the mid stratosphere.

4. The depth of the PV anomalies

The PV anomalies which arise in the high stratosphere reach a depth of maximally 450K in (roughly 50-100 hPa) in these cases. That is still in the low stratosphere, so the PV-anomalies do not enter the troposphere and could not directly influence the general tropospheric circulation. However, as explained in section 2.2.4, a PV anomaly can have a influence in a certain vertical range (the Rossby scale height). In field theories, this principle is called 'action at a distance': it states that two or more objects can exert a net force on each other without being in physical contact. This 'action at a distance' also holds for PV anomalies. Like electric charges can influence each other by inducing an electric field, a PV anomaly can influence the troposphere without intersecting the troposphere.

Going back to the Rossby scale height, it can be noticed first that the estimated value of 225K of the Rossby height for a PV anomaly at the 850K level is lower than the Rossby height in the cases: during phases of positive PV anomalies before the SSW, the Rossby height is often more than 350K and during the phases with a negative anomaly more than 250K. For PV anomalies at the 500K level, the Rossby height lies around 180K for positive PV anomalies before the SSW and 130K for negative PV anomalies.
For the SSW and DSW of 2019, the negative PV anomalies do not reach very deep: mostly around 600K with a short peak to 500K. This can also be seen in the Rossby height for this case: they are lower compared to the other cases during the phase of negative PV anomaly. This may explain the weak tropospheric reaction that year: the PV anomalies and its maximum vertical range were insufficient to affect the troposphere strongly.

5. The increase of the total mass flux

As found in every case, the poleward mass flux increases during an SSW, and ceases generally in the some days after the DSW. This increased poleward mass flux in the middle stratosphere is mostly due to an increased eddy mass flux. This poleward mass flux is also present in the lower stratosphere, but is then mostly dominated by an enhanced mean circulation (not for all cases). This is contradictory to what Cai and Ren found in their paper, in which it was stated that at lower heights there should be a compensating equatorward mass flux. A reason for this might be that the evaluated region is still to high; the compensating mass flux takes place lower. In appendix C, tables of the net mass flux at each level are given. In every case, the mass flux is equatorwards in the lowest layers in the troposphere. This corresponds to Cai and Rens mass paradigm.

6. The anticorrelation between mass and PVS flux

As seen in the results section, the total accumulative mass and PVS flux are pretty well anticorrelated with each other: if the total mass flux increases, the total PVS flux decreases. In the end, the net total PVS flux is negative (southward). This is partially due to the (anti)correlation of isentropic mass and PVS to PV-anomalies. It can be easily seen from the definition of potential vorticity that a positive PV anomaly correlates negatively with (anomalies of) isentropic mass and positively with (anomalies of) PVS.

However, in the lower stratosphere, this anticorrelation is less visible and sometimes even not present. A reason for this might be that the PV anomalies do not always reach this level long enough. There exists no correlation at this level since there are no PV anomalies. The evolution of the mass and PVS flux might have another external factor, such as diabatic forcings.

7. The eddy and mean circulation fluxes and their anticorrelation

The eddy and mean circulation fluxes have mostly the opposite behavior. For the PVS flux, this pattern is visible in both integrated layers. This pattern can be explained by the impermeability theorem, which states that isentropes are impermeable to PVS: PVS can not flow through isentropes (see section 2.2.2). The net sum of the PVS flux along an isentrope must therefore be zero, so the eddy and mean circulation fluxes must eventually compensate each other. In other words: an increased eddy flux brings the atmosphere out of its

zonal mean state and the compensating mean circulation flux brings the atmosphere back to its zonal mean state. This is the balance response between the eddy PVS flux and mean circulation pvs flux. Considering the isentropic mass flux, the same compensating behavior of the eddy and mean circulation components can be seen in the 600-850K layer (middle stratosphere). However, in the 395-530K layer (lower stratosphere), this anticorrelation does not hold. This is clearly visible in the cases of 2009 and 2013: there are periods where both the eddy and mean circulation flux increase or decrease. A reason for this may be that in in the lower stratosphere, diabatic effects such as latent heat release (second term on the r.h.s of equation (7)) might become important (isentropes are permeable to mass under diabatic circumstances (equation 8)). The compensation behavior of the isentropic eddy mass flux and mean circulation flux is an indication that the creation of negative PV anomalies during SSWs is explained by advection of isentropic mass, which is also a sign of an increased mass circulation.

The fast increase (decrease) of the mass (PVS) during and after a SSW and DSW is an indication of the response of an atmosphere which is perturbed from its zonal mean balanced state. When the change of mass and PVS has ceased, the atmosphere has adjusted to the perturbation and reached its steady state again. This is visible in all figures of the accumulative fluxes integrated between 600-850K. In the lower stratosphere, this response sets in on a later time, depending on how far the negative PV anomalies and the Rossby height stretch.

8. Changes in static stability

In practically all cases, we see that the static stability at 850K drops after a SSW and that it later happens at lower levels. This can be easily explained by one of the definitions of potential vorticity: it scales with the static stability as $\mathcal{P}N^2$ (equation 5). The isentropic mass naturally scales too with the static stability as $\sigma\tilde{1}/N^2$. Since negative PV anomalies correspond with positive mass anomalies, the static stability obeys the same relation. What physically happens is that more mixing of mass takes place which destroys the stratification, weakening and destructing the polar vortex eventually. When the atmosphere returns back to its zonal mean state, the stratification in the stratosphere restores. The polar vortex returns back to its original state.

5.2 Additional discussion points

The initial state of the atmosphere

Although a number of similarities which may provide an explanation of the downward effects of stratospheric warmings were found, the exact tropospheric response is still variable. There is one thing which is not mentioned yet: the role of the initial state of both the troposphere and the polar vortex. For example, in 1985, the atmosphere was already pretty blocked 15 days before the SSW. There was a huge tropospheric impact some weeks later. This is also slightly the case for 2009. It may be possible that if an atmosphere which is or was already blocked in the weeks before the SSW, gets more easily blocked when the effects of the SSW/DSW sets in. Before the SSW takes place, the tropospheric circulation is already perturbed. The effects coming from an SSW could make it then easier to block the atmosphere more and subsequently, let the AO and NAO become smaller or negative. Of course, it does not mean that if the initial state of the atmosphere is not (semi)-blocked, that the tropospheric impact can not be huge: 2018 is an example of that.

Quasi-geostrophic PV view versus $PV-\theta$ view

In the most papers about the stratosphere and stratospheric influence, the calculations and simulations are done in the quasi-geostrophic PV view. The PV-theta view is not used a lot yet. It is therefore hard to compare the results of this thesis to that of the most available papers. A drawback of the quasi-geostrophic PV view is that it lacks the evolution of mass, which is important in the $PV-\theta$ view. It explains the evolution of meridional mass circulations. The one which comes the closest to the $PV-\theta$ view is the mass-paradigm from Cai and Ren. They evaluated the different parameters on planes of constant PV. As shown in appendix C, this principle holds. Also the role of vorticity is discussed, although not in the PVS form and its effect on the zonal wind.
It does naturally not mean that the quasi-geostrophic PV view is worthless. The mathematical formalism of the vertically propagating planetary waves is a result of perturbed quasi-geostrophic PV theory and as explained, these waves partially transport and mix PV, which is an important aspect of the onset of SSWs as well as the downward propagation later.

With the $PV-\theta$ view, some observations and results found in earlier studies can be explained, like the changes in the AO and NAO, and the weakening and meandering of the polar jet stream.

6 Conclusion

The goal of this thesis was to get more insight into how perturbations in the stratosphere, induced by an SSW, can change the tropospheric circulation and how the $PV-\theta$ view can give an explanation of this effects. These perturbations have to travel a long vertical distance in order to disturb the tropospheric circulation. The key mechanism is the adjustment of the zonal mean state of the stratosphere and troposphere to thermal wind balance. In the $PV-\theta$ view, the potential temperature and potential vorticity are the most important parameters. The PV-equation describes the change of PV and the formation of PV anomalies. The PV-invertibility equation is an expression of the thermal wind balance. PV anomalies induce a zonal wind which is eastward or westward, depending on the sign of the PV anomaly. Redistribution of PV (and creation of PV anomalies) is caused by planetary wave breaking and a changed strength of the flux of isentropic mass and PVS: a positive PV anomaly is the result of a negative anomaly of the isentropic mass and a positive anomaly of PVS. Redistribution of PV leads to adjustment of zonal mean state to thermal wind balance. An SSW is an extreme case of this PV-mixing. When an SSW is deep enough and the criteria of a DSW are satisfied, the chance that it affects the tropospheric circulation increases. Actually, the date of the DSW is the date were already tropospheric impact can be expected.

During an SSW, the poleward flux of isentropic mass increases, leading to a negative PV anomaly in the stratosphere and an increased pressure. According to Kleinschmidts principle, the air mass loses the property of a cold air mass and the air warms up and sinks. The polar jet at $60°N$ is an eddy-driven jet. The equatorward PVS flux in the lower stratosphere/upper troposphere 'exerts a force' on the polar jet which causes the jet to decelerate.

PV anomalies formed during an SSW and DSW never reach the troposphere. The PV anomalies may still have a tropospheric impact due to its long vertical extent, called the Rossby scale height. The Rossby height depends on the static stability of the air mass. The static stability changes when the stratification in the stratosphere is disturbed. The negative PV anomalies during an SSW can still exert their influence on the troposphere if the Rossby height is large enough, according to the action at a distance principle. For a DSW, there is a higher probability that the tropospheric circulation gets affected.

Summarized, the $PV-\theta$ provides insight into the downward effects of SSW by redistribution of PV and subsequent formation of PV anomalies. These PV anomalies lead to adjustment of the zonal mean state of the atmosphere to thermal wind balance, as explained by the PV-inversion equation. The PV anomalies have a vertical reach which may be sufficiently large to affect the tropospheric circulation.

7 Further outlook

Of course, not every aspect of the downward propagation of SSW effects is explained. In this thesis, the role of diabatic effects is mainly neglected, which may become important, especially in the lower stratosphere.

For further research, it may be useful to consider the evolution of the concentration of ozone during a SSW event. There are two reasons to do this: it may give a more detailed view of the changes in the mass circulation and it can be used to make an estimation of the diabatic terms in the PV-equation. That can give more insight into the long-wave radiation balance which might be an important factor for both the cause of the SSW and the tropospheric influence. The role of water can also be researched.

The stratosphere is a part of a complex and coupled system. There are connections with the troposphere clearly. In some papers on the stratosphere and SSWs, the role of the quasi-biennal oscillation (QBO) and the sunspot cycle is discussed. The QBO is the oscillation of positive and negative equatorial zonal winds. It has a period of approximately two years. It is proposed that a negative phase of the QBO promotes the occurence of SSWs and may also disturb the troposphere. The solar cycle can be of significant importance for the radiation balance: during the maximum phase of the solar cycle, more UV-radiation is emitted by the sun. Periods of low solar activity are linked to a more negative phase of the (N)AO. These two parameters can also be important for the initial state of the tropospheric circulation.

These are just two examples of external factors which may influence the evolution of an SSW. There are undoubtedly more factors which may be of great importance for SSW studies. In this thesis, the puzzle pieces of a SSW are provided using the $PV-\theta$ framework; now the puzzle pieces have to be put together, which can be done by numerical simulations of the PV equation and PV-invertibility equation.

Appendices

A Derivation of the PV-inversion equation

In this appendix, a derivation of the PV-inversion equation is provided. The goal of this derivation is to show that the PV-inversion equation is a statement of the principle of thermal wind, expressed in potential vorticity. First, remind the definition of potential vorticity:

$$\mathcal{P} = -g(\zeta + f)\frac{\partial \theta}{\partial p} = \frac{\zeta + f}{\sigma}, \tag{24}$$

$$\zeta = \frac{\partial v}{\partial x} - \frac{\partial u}{\partial y}; f = 2\Omega \sin\phi; \sigma = -\frac{1}{g}\frac{\partial p}{\partial \theta}; \theta = T(\frac{p_{ref}}{p})^{\kappa},$$

where $\mathcal{P}$ is the potential vorticity, ζ the relative vorticity, f the Coriolis parameter, θ the potential temperature, p the pressure, T the temperature, $\kappa = \frac{R}{c_p}$ the ratio of the air gas constant to the specific heat capacity of air and g the gravitational acceleration.
Now, let's convert some basic equations to isentropic coordinates (with the potential temperature θ as the vertical coordinate), beginning with the horizontal momentum equations without friction:

$$\frac{du}{dt} = \frac{\partial u}{\partial t} + u\frac{\partial u}{\partial x} + v\frac{\partial u}{\partial y} + \frac{d\theta}{dt}\frac{\partial u}{\partial \theta} = -\frac{\partial \psi}{\partial x} + fv + \frac{uv\tan\phi}{a}, \tag{25a}$$

$$\frac{dv}{dt} = \frac{\partial v}{\partial t} + u\frac{\partial v}{\partial x} + v\frac{\partial v}{\partial y} + \frac{d\theta}{dt}\frac{\partial v}{\partial \theta} = -\frac{\partial \psi}{\partial x} - fu + \frac{u^2\tan\phi}{a}. \tag{25b}$$

The first term on the right-hand side denotes the pressure gradient force, the second term the Coriolis effect and the third term the centrifugal effect, where a is the Earths radius. The Montgomery stream function ψ is defined by:

$$\psi = c_p T + gz = \theta\Pi + gz, \tag{26}$$

z denotes here the height of the isentropic surface. Also

$$\Pi = c_p(\frac{p}{p_{ref}})^{\kappa} = c_p\frac{T}{\theta} \tag{27}$$

is the Exner function. The hydrostatic balance is terms of the Exner function is:

$$\frac{\partial \Pi}{\partial z} = -\frac{g}{\theta}, \tag{28}$$

By taking the derivative of the Montgomery streamfunction with respect to z, the hydrostatic balance can also be expressed as:

$$\frac{\partial \psi}{\partial \theta} = \Pi \tag{29}$$

Next step is to write down the gradient wind balance (du/dt = dv/dt = 0):

$$\frac{u^2\tan\phi}{a} = -\frac{\partial \psi}{\partial y} - fu \tag{30a}$$

$$\frac{uv\tan\phi}{a} = -\frac{\partial \psi}{\partial x} + fv \tag{30b}$$

These are the basic equations in isentropic coordinates. From now on, we will focus on only the zonal component (equation 30a) because in this study, only the zonal wind is of importance. Furthermore, we take

the zonal mean, denoted between square brackets, of it. For example, the zonal mean of the potential vorticity is:

$$[\mathcal{P}] = [\frac{\zeta + f}{\sigma}] \approx \frac{[\zeta] + f}{[\sigma]}. \tag{31}$$

The zonal mean of the relative vorticity is:

$$[\zeta] = \frac{[u]\tan\phi}{a} - \frac{\partial[u]}{\partial y}. \tag{32}$$

Differentiating (31) with respect to y gives:

$$\begin{aligned}
&\frac{\partial[\mathcal{P}]}{\partial y} = \frac{1}{[\sigma]}\frac{\partial([\zeta]+f)}{\partial y} + ([\zeta]+f)\frac{\partial([\sigma]^{-1})}{\partial y} = \frac{1}{[\sigma]}(\frac{\partial[\zeta]}{\partial y} + \frac{\partial f}{\partial y}) - \frac{[\mathcal{P}]}{[\sigma]^2}\frac{\partial\sigma}{\partial y} \\
&= \frac{1}{[\sigma]}(\frac{\partial[\zeta]}{\partial y} + \frac{\partial f}{\partial y}) - \frac{[\mathcal{P}]}{[\sigma]^2}\frac{\partial}{\partial y}(-\frac{1}{g}\frac{\partial[p]}{\partial\theta}) = \frac{1}{[\sigma]}(\frac{\partial[\zeta]}{\partial y} + \frac{df}{dy}) + \frac{[\mathcal{P}]}{[\sigma]}\frac{\partial}{\partial\theta}(\frac{\partial[p]}{\partial y})
\end{aligned}$$

$$\Rightarrow \boxed{[\sigma]\frac{\partial[\mathcal{P}]}{\partial y} = \frac{\partial[\zeta]}{\partial y} + \frac{\mathcal{P}}{[\sigma]g}\frac{\partial}{\partial\theta}(\frac{\partial[p]}{\partial y}) + \frac{df}{dy}}. \tag{33}$$

Next, we derive the thermal wind equation in isentropic coordinates. To do this, take the derivative of (the zonal mean) equation (29) (hydrostatic balance) with respect to y and the derivative of (30a) (gradient wind) with respect to θ and subtract:

$$\begin{aligned}
\frac{\partial}{\partial y}(29) &= \frac{\partial^2[\psi]}{\partial y\partial\theta} = \frac{\partial[\Pi]}{\partial y}, \\
\frac{\partial}{\partial\theta}(30a) &= \frac{2[u]\tan\phi}{a}\frac{\partial[u]}{\partial\theta} = -\frac{\partial}{\partial\theta}\frac{\partial\psi}{\partial y} - f\frac{\partial[u]}{\partial\theta} \\
\Rightarrow \frac{\partial^2[\psi]}{\partial y\partial\theta} - \frac{\partial^2[\psi]}{\partial\theta\partial y} &= \frac{\partial[\Pi]}{\partial y} + (f + \frac{2[u]\tan\phi}{a})\frac{\partial[u]}{\partial\theta} = 0
\end{aligned}$$

$$\Rightarrow \boxed{f_{loc}\frac{\partial[u]}{\partial\theta} = -\frac{\partial[\Pi]}{\partial y}}, \tag{34}$$

where $f_{loc} = f + \frac{2[u]\tan\phi}{a}$. It states that the vertical gradient (remember that θ is the vertical coordinate) of [u] is proportional to the meridional gradient of the temperature (Remember that the Exner function is a function of T). Taking the derivative of the Exner function (expressed in p) with respect to y and using the ideal gas law gives:

$$\frac{\partial[\Pi]}{\partial y} = c_p\kappa\frac{[p]^{\kappa-1}}{p_{ref}^{\kappa}}\frac{\partial[p]}{\partial y} = \frac{c_p\kappa}{[p]}(\frac{p}{p_{ref}})^{\kappa}\frac{\partial p}{\partial y} = \frac{c_p}{R[\rho][T]}\frac{R}{c_p}\frac{[T]}{\theta}\frac{\partial[p]}{\partial y} = \frac{1}{[\rho]\theta}\frac{\partial[p]}{\partial y}$$

$$\Rightarrow \frac{\partial[\Pi]}{\partial y} = \frac{1}{[\rho]\theta}\frac{\partial[p]}{\partial y}, \tag{35}$$

where ρ is the density of air. Plugging equation (35) into (34) gives then:

$$\boxed{-\frac{\partial[p]}{\partial y} = f_{loc}\theta[\rho]\frac{\partial[u]}{\partial\theta}}. \tag{36}$$

This is still the thermal wind balance, but then expressed in terms of a meridional pressure gradient. Finally, by plugging in equation (36) (thermal wind) and (32) (relative vorticity) into equation (33) (meridional gradient of potential vorticity) gives:

$$-\frac{\partial}{\partial y}(-\frac{\partial [u]}{\partial y}+[u]\frac{\tan\phi}{a})+\frac{[\mathcal{P}]}{[\sigma]g}\frac{\partial}{\partial\theta}(-f_{loc}\theta[\rho]\frac{\partial [u]}{\partial\theta})=\frac{df}{dy}-[\sigma]\frac{[\mathcal{P}]}{\partial y}$$

$$\Rightarrow \boxed{\frac{\partial}{\partial y}(\frac{\partial [u]}{\partial y}-[u]\frac{\tan\phi}{a})+\frac{[\mathcal{P}]}{[\sigma]g}\frac{\partial}{\partial\theta}(f_{loc}\theta[\rho]\frac{\partial [u]}{\partial\theta})=\frac{df}{dy}-[\sigma]\frac{\partial[\mathcal{P}]}{\partial\theta}}. \tag{37}$$

This equation is called the potential vorticity inversion equation. As shown, it states in fact the thermal wind equation expressed in isentropic coordinates in terms of the meridional potential vorticity gradient. Remember that this equation holds for the zonal component of the wind.

B Derivation of the Rossby scale height in terms of the static stability

In this appendix, the expression for the Rossby scale height in terms of the static stability parameter will be derived. In section 4.2.3, it was found that Rossby scale height expressed in potential (equation (14)) is:

$$\boxed{\Delta\theta=\sqrt{\frac{L^2 f_{ref}\theta\mathcal{P}_{ref}\rho}{4\pi^2 g^2}}}. \tag{38}$$

The first step is to insert the isentropic density σ into equation (38), and expanding it by using the definition of σ:

$$\Delta\theta=\sqrt{\frac{L^2 f_{ref}\theta\mathcal{P}_{ref}\rho}{4\pi^2 g^2}}=\frac{L}{2\pi}\sqrt{\frac{f\mathcal{P}\theta}{g\sigma}\rho\sigma}=\frac{L}{2\pi}\sqrt{\frac{f\mathcal{P}\sigma\theta}{g}-\rho g\frac{\Delta\theta}{\Delta P}}. \tag{39}$$

The next step is to make use of the hydrostatic balance to eliminate the pressure:

$$\frac{L}{2\pi}\sqrt{f\mathcal{P}\sigma\theta-\rho\frac{\Delta\theta}{\Delta P}}=\frac{L}{2\pi}\sqrt{f\mathcal{P}\sigma\theta\frac{-\rho\Delta\theta}{-g\rho\Delta z}}=\frac{L}{2\pi}\sqrt{\frac{f\mathcal{P}\sigma\theta}{g}\frac{\Delta\theta}{\Delta z}}, \tag{40}$$

where $\sigma=\eta+f$. Equation (40) can now be rewritten as:

$$\frac{L}{2\pi}\sqrt{\frac{f\mathcal{P}\sigma\theta}{g}\frac{\Delta\theta}{\Delta z}}=\frac{L}{2\pi}\sqrt{\frac{f(\eta+f)\theta}{g}\frac{\Delta\theta}{\Delta z}}=\frac{L}{2\pi}\sqrt{\frac{F^2 g\theta^2}{\theta g^2}\frac{\Delta\theta}{\Delta z}}=\frac{L}{2\pi}\sqrt{F^2N^2}\frac{\theta}{g}, \tag{41}$$

where $N^2=\frac{g}{\theta}\frac{\Delta\theta}{\Delta z}$. So in the end, the Rossby scale height in terms of the static stability is:

$$\Rightarrow \boxed{\Delta\theta=\frac{L\theta}{2\pi g}FN}. \tag{42}$$

C Supplementary tables

Table 2: Total accumulative mass and PVS flux on Central Date and final day in mid stratosphere (600-850K) for each case

Year	$[v\sigma]_{CD}(kg/m/s/K)$	$[v\sigma]_{end}(kg/m/s/K)$	$[vPVS]_{CD} * 10^{-3}(1/s^2)$	$[vPVS]_{end} * 10^{-3}(1/s^2)$
1985	35.6	46.4	-1.29	-1.47
2009	49.0	70.9	-4.16	-3.61
2013	21.4	30.0	-3.67	-6.00
2018	27.8	29.2	-2.40	-2.70
2019	21.5	33.2	-2.22	-2.40

Table 3: Total accumulative mass and PVS flux on Central date and final day in the low stratosphere (395-530K) for each case.

Year	$[v\sigma]_{CD}(kg/m/s/K)$	$[v\sigma]_{end}(kg/m/s/K)$	$[vPVS]_{CD} * 10^{-3}(1/s^2)$	$[vPVS]_{end} * 10^{-3}(1/s^2)$
1985	141.3	250.7	-2.91	-0.81
2009	158.9	322.9	-3.27	-2.01
2013	197.9	291.3	-0.14	1.10
2018	231.9	354.3	-0.03	0.48
2019	190.2	310.0	1.90	2.72

Table 4: Accumulative mass and PVS flux on isentropes in January 1985.

θ-level	$[v\sigma]_{end}(kg/m/s/K)$	$[vPVS]_{end} * 10^{-3}(1/s^2)$
850	14.2	-0.36
700	25.2	-0.48
600	28.1	-1.61
530	89.0	0.15
475	112.6	-0.74
430	125.3	0.49
395	-63.3	-1.28
370	-5.8	-0.39
350	36.1	-0.85
330	275.2	0.21
320	258.0	-0.35
315	1012.8	-0.57
300	8888.3	0.24
285	12676.2	-0.43
275	-21375.4	-10.14
265	-8783.2	-17.47

Table 5: Accumulative mass and PVS flux on isentropes in January 2009.

θ-level	$[v\sigma]_{end}(kg/m/s/K)$	$[vPVS]_{end} * 10^{-3}(1/s^2)$
850	13.0	-1.79
700	39.8	-1.67
600	49.2	-2.07
530	66.9	-1.25
475	61.9	-1.38
430	132.7	-0.15
395	190.2	0.14
370	122.1	-0.20
350	134.7	0.20
330	88.9	-0.28
320	434.6	0.04
315	2528.0	0.11
300	11780.4	-0.35
285	11612.2	-0.45
275	-12447.4	-6.46
265	-4813.0	-8.65

Table 6: Accumulative mass and PVS flux on isentropes in January 2013.

θ-level	$[v\sigma]_{end}(kg/m/s/K)$	$[vPVS]_{end} * 10^{-3}(1/s^2)$
850	10.1	-0.52
700	14.2	-3.00
600	21.6	-2.41
530	48.5	-0.66
475	30.7	-0.96
430	159.4	1.84
395	153.8	1.18
370	98.5	0.37
350	-17.1	-0.43
330	178.4	0.21
320	924.5	0.12
315	2953.4	-0.13
300	8900.8	-0.26
285	7195.5	-0.31
275	-12780.0	-7.81
265	-6713.4	-12.01

Table 7: Accumulative mass and PVS flux on isentropes in February 2018.

θ-level	$[v\sigma]_{end}(kg/m/s/K)$	$[vPVS]_{end} * 10^{-3}(1/s^2)$
850	17.4	0.95
700	8.5	-1.89
600	24.1	-1.01
530	30.9	-0.55
475	79.7	-0.35
430	185.1	1.05
395	148.2	0.11
370	175.8	0.63
350	142.0	0.81
330	80.0	0.44
320	552.0	0.19
315	1589.2	0.01
300	4865.0	-0.07
285	3713.8	-0.05
275	-14397.5	-4.74
265	-15755.0	-8.91

Table 8: Accumulative mass and PVS flux on isentropes in January 2019.

θ-level	$[v\sigma]_{end}(kg/m/s/K)$	$[vPVS]_{end} * 10^{-3}(1/s^2)$
850	8.7	0.24
700	20.4	-1.25
600	16.7	-2.54
530	41.2	-1.44
475	86.0	0.55
430	174.7	2.58
395	57.5	0.63
370	0.6	0.00
350	-4.7	-0.16
330	-26.2	-0.67
320	-14181.7	-0.28
315	13074.0	-0.33
300	35759.4.0	-0.34
285	3713.8	-0.46
275	404.3	-2.96
265	-2650.1	-6.81

References

[1] Geoffrey K. Vallis, 2017: *Atmospheric and Oceanic fluid dynamics*, 599-609

[2] Ian N. James, 1995: *Introduction on circulating atmospheres*, 190-204

[3] Nath. D et al., 2016: Dynamics of 2013 Sudden Stratospheric Warming event and its impact on cold weather over Eurasia: Role of planetary wave reflection, *Sci. Rep.6*, 24174, 1-12

[4] J. T. Abatzoglou and G. Magnusdottir, 2007: Wave breaking along the stratospheric polar vortex as seen in ERA-40 data, *Geophys. Res. Lett*, 34, 1-5

[5] Butler et al., 2017: A sudden stratospheric warming compendium, *Earth Syst. Sci. Data*, 9, 63-76

[6] M. Cai and R.-C. Ren, 2006: Meridional and Downward Propagation of Atmospheric Circulation Anomalies. Part I: Northern Hemisphere Cold Season Variability, *J. Atmos.Sci.*, 64, 1880-1901

[7] Lars van Galen, 2018: *Sudden Stratospheric Warmings developing a new classification based on vertical depth, applying theory to a SSW in 2018 and assessing predictability of a cold air outbreak following this SSW (master thesis report)*

[8] Blanca Ayarzagena et al., 2019: On the representation of major stratospheric warmings in reanalyses, *Atmos. Chem. Phys.*, 19, 9469-9484

[9] M.P. Baldwin and T.J. Dunkerton, 1999: Propagation of the Arctic Oscillation from the stratosphere to the troposphere, *J. Geophys. Res.*, 104, 36937-30946

[10] M.P. Baldwin and T.J. Dunkerton, 2001: Stratospheric Harbingers of Anomalous Weather Regimes, *Science*, 294, 581-584

[11] J. Kidston et al., 2015: Stratospheric influence on tropospheric jet streams, storm tracks and surface weather, *Nature GeoScience*, 8, 433-440

[12] Aarnout van Delden, 2018: *The general circulation of the atmosphere lecture notes*, 55-68

[13] Aarnout van Delden and Yvonne Hinssen, 2012: PV-θ view of the zonal mean state of the atmosphere, *Tellus A: Dynamic Meteorology and Oceanography*, 64, 1-17

[14] Jonathan E. Martin, 2006: *Mid-Latitude Atmospheric Dynamics: A first course*, 280-282

[15] A. Thorpe, 2002: Extratropical cyclones an historical perspective, *Int. Geophys.*, 83, 14-22

[16] P.H. Haynes and M.E. McIntyre, 1990: On the conservation and impermeability theorems for potential vorticity, *J. Atmos. Sci.*, 47, 2021-2031

[17] Aarnout van Delden, 2017: *Atmospheric Dynamics lecture notes*, 216-224

[18] Steven M. Cavallo and Gregory John Hakim, 2010: Composite Structure of Tropopause Polar Cyclones, *J. Atmos. Sci.*, 138, 3840-3857

[19] Copernicus Climate Change Service (C3S) (2017): ERA5: Fifth generation of ECMWF atmospheric reanalyses of the global climate . Copernicus Climate Change Service Climate Data Store (CDS), 2018-2019. https://cds.climate.copernicus.eu/cdsapp!/home

[20] Aarnout van Delden, 2017: *Atmospheric Dynamics lecture notes*, 141-142

[21] John P. Snyder, 1987: *Map Projections - A Working Manual*, 1395, 145-153

[22] National oceanic and atmospheric administration et al., 1976:*U.S. Standard Atmosphere 1976*, 50-73